Ionosphere Response to the simultaneous and consecutive occurrence of Geomagnetic Storm and Lightning at various intensities in a Low Latitude Region

Louis Osei-Poku[1], WU CHEN[2], Mingli Chen[2], Tang Long[3], and Akwasi Acheampong Afrifa[4]

[1]Department of Land Surveying and Geo-Informatics, The Hong Kong Polytechnic University, Kowloon, Hong Kong
[2]Hong Kong Polytechnic University
[3]School of Civil and Transportation Engineering, Guangdong University of Technology
[4]Geomatic Eng. Dept., KNUST

December 22, 2022

Abstract

Information from total electron content (TEC) from Global Navigation Satellite Systems (GNSS) could be assessed to know the impact of weather events to help in developing prediction and warning systems. The majority of studies focus on the occurrence of only one event neglecting situations where these weather events happen almost simultaneously or consecutively. This current study tends to fill the gap by analyzing ionosphere response following the simultaneous and/or consecutive occurrence of geomagnetic storm and lightning events at various intensities in southern China coastal region. The results showed that the magnitude of the frequency lightning-related events using continuous wavelet transform (CWT) was 0.3-0.4 while that of geomagnetic storm was 0.15-0.3. However, the various levels of intensity could not be distinguished. Being able to differentiate the weather events by the magnitude values following the ionosphere response is good for prediction and modeling purposes as the use of TEC in some studies does not provide this clear distinction.

Hosted file

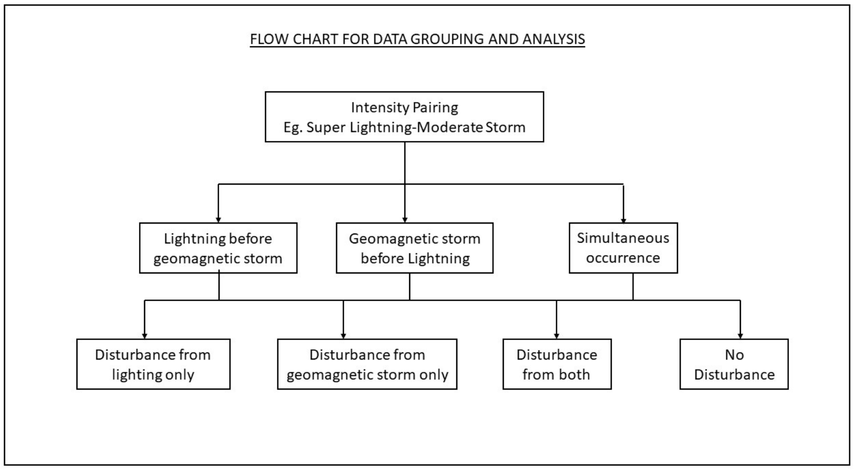
FLOW CHART FOR DATA GROUPING AND ANALYSIS
Intensity Pairing
Eg. Super Lightning-Moderate Storm
Lightning before geomagnetic storm
Geomagnetic storm before Lightning
Simultaneous occurrence
Disturbance from lighting only
Disturbance from geomagnetic storm only
Disturbance from both
No Disturbance

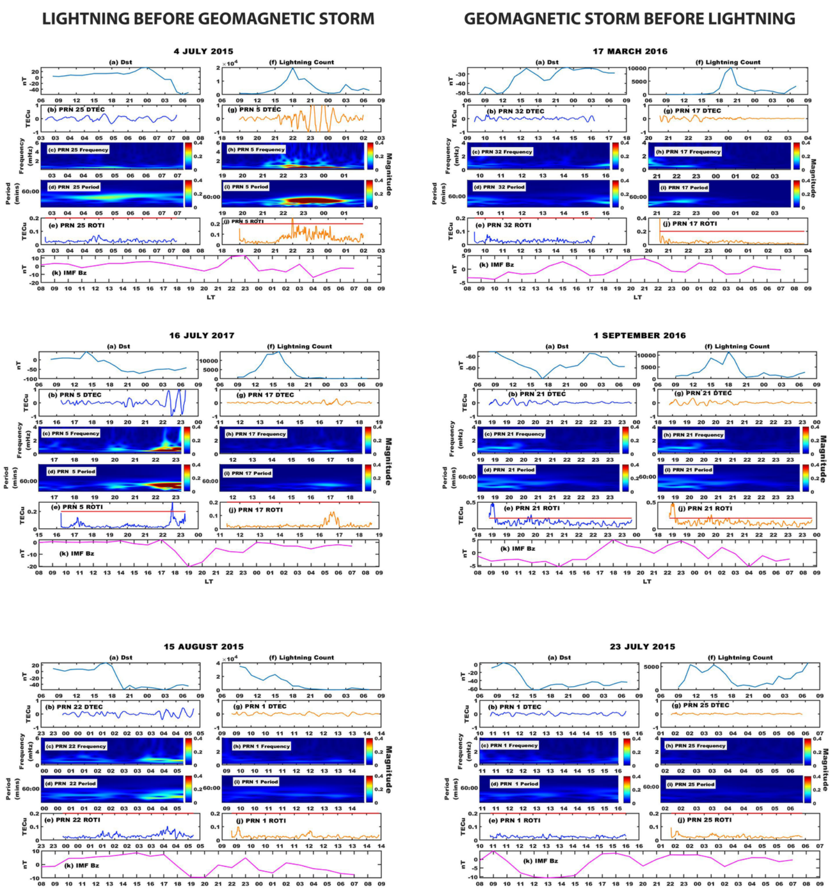
LIGHTNING BEFORE GEOMAGNETIC STORM
GEOMAGNETIC STORM BEFORE LIGHTNING
4 JULY 2015
17 MARCH 2016
16 JULY 2017
1 SEPTEMBER 2016
15 AUGUST 2015
23 JULY 2015
(a) Dst
(f) Lightning Count
(k) IMF Bz
Magnitude
LT

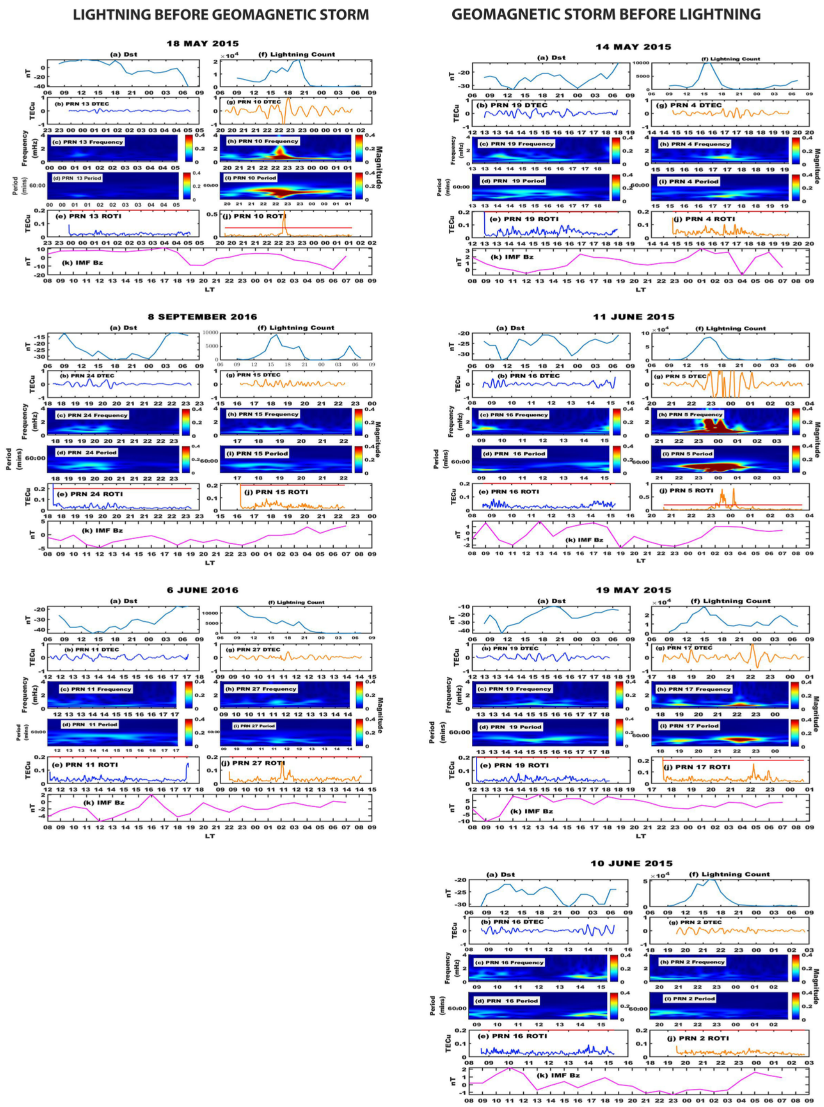
LIGHTNING BEFORE GEOMAGNETIC STORM
GEOMAGNETIC STORM BEFORE LIGHTNING
18 MAY 2015
14 MAY 2015
8 SEPTEMBER 2016
11 JUNE 2015
6 JUNE 2016
19 MAY 2015
10 JUNE 2015
(a) Dst
(f) Lightning Count
(k) IMF Bz
LT
Magnitude

SUPER LIGHTNING - NO GEOMAGNETIC STORM (SL-NS)

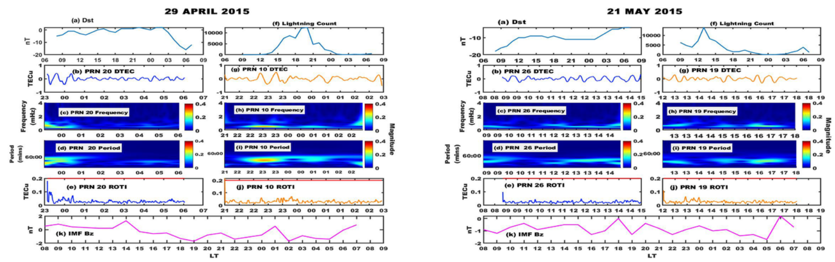

INTENSE LIGHTNING - NO GEOMAGNETIC STORM (IL-NS)

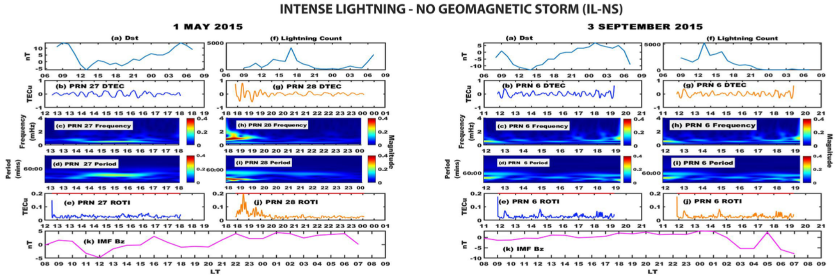

MODERATE LIGHTNING - NO GEOMAGNETIC STORM (ML-NS)

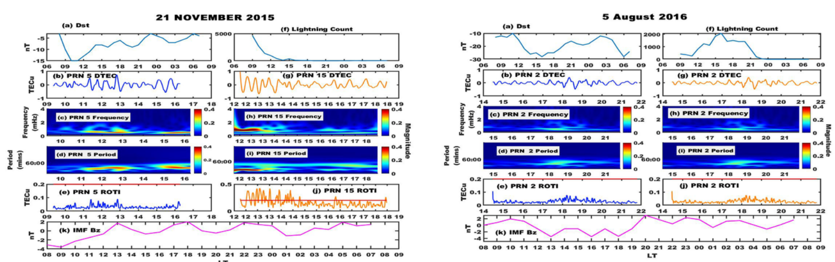

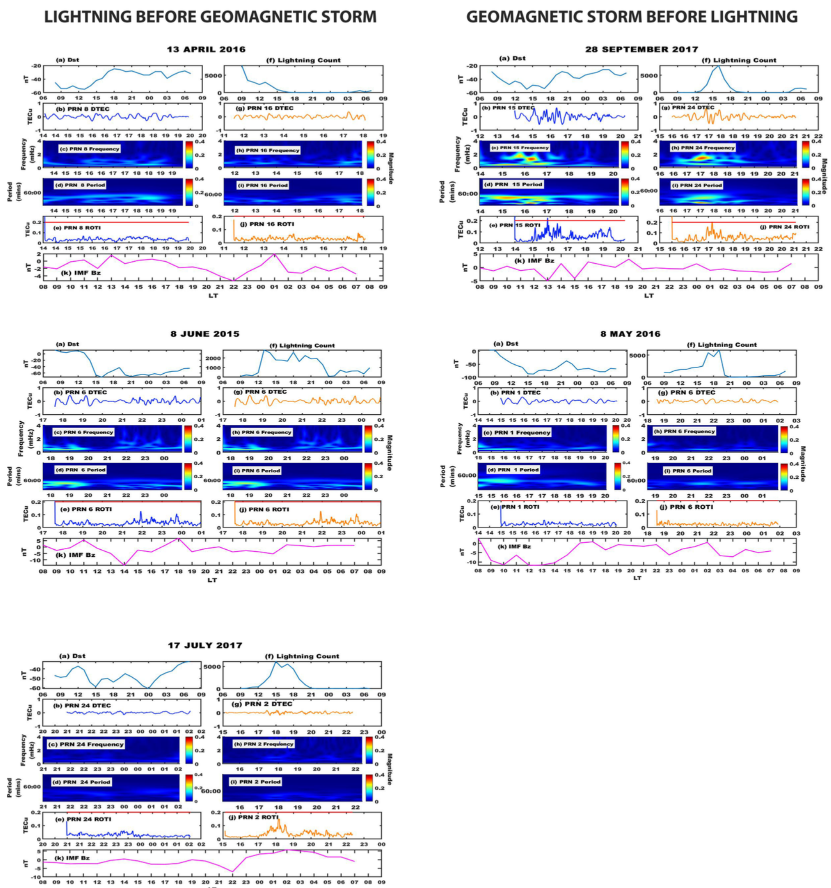
LIGHTNING BEFORE GEOMAGNETIC STORM
GEOMAGNETIC STORM BEFORE LIGHTNING
13 APRIL 2016
28 SEPTEMBER 2017
8 JUNE 2015
8 MAY 2016
17 JULY 2017
(a) Dst
(f) Lightning Count
(b) PRN 8 DTEC
(g) PRN 16 DTEC
(c) PRN 8 Frequency
(h) PRN 16 Frequency
(d) PRN 8 Period
(i) PRN 16 Period
(e) PRN 8 ROTI
(j) PRN 16 ROTI
(k) IMF Bz
Magnitude
LT

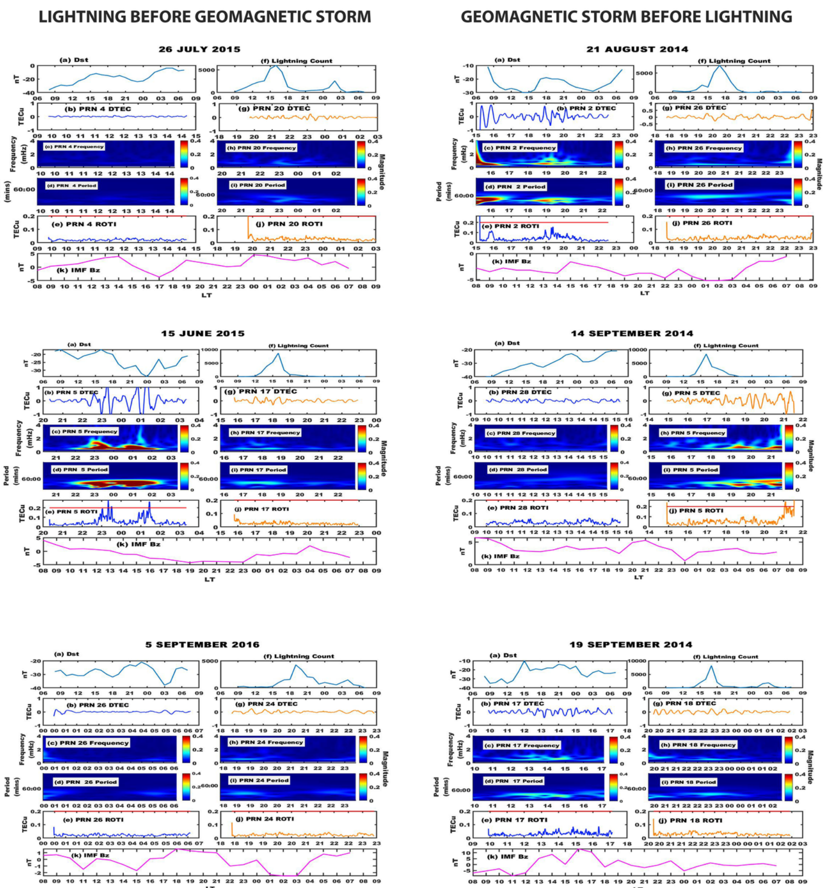
LIGHTNING BEFORE GEOMAGNETIC STORM
GEOMAGNETIC STORM BEFORE LIGHTNING
26 JULY 2015
21 AUGUST 2014
15 JUNE 2015
14 SEPTEMBER 2014
5 SEPTEMBER 2016
19 SEPTEMBER 2014
(a) Dst
(f) Lightning Count
(k) IMF Bz
LT

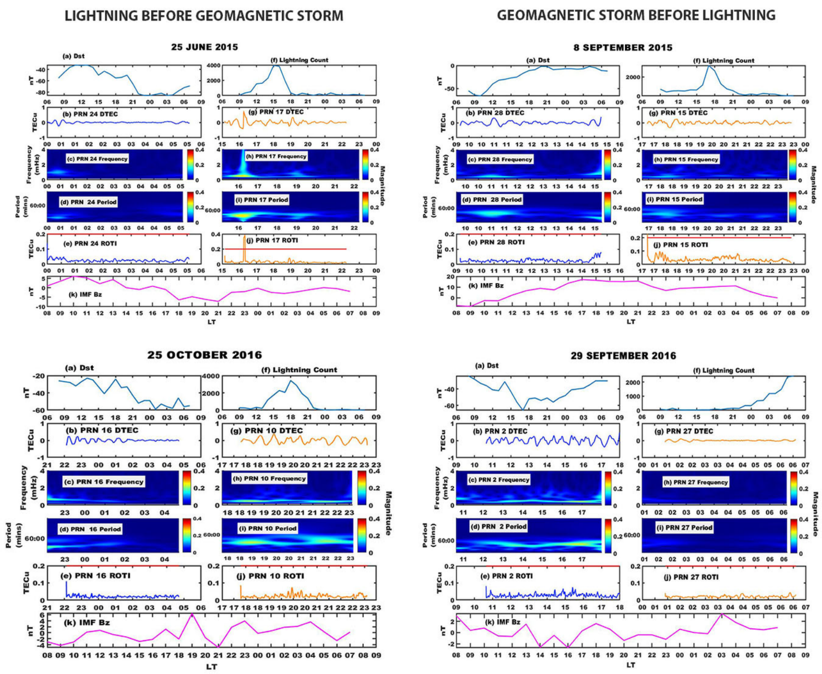
LIGHTNING BEFORE GEOMAGNETIC STORM
GEOMAGNETIC STORM BEFORE LIGHTNING
25 JUNE 2015
8 SEPTEMBER 2015
25 OCTOBER 2016
29 SEPTEMBER 2016
(a) Dst
(f) Lightning Count
(b) PRN 24 DTEC
(g) PRN 17 DTEC
(c) PRN 24 Frequency
(h) PRN 17 Frequency
(d) PRN 24 Period
(i) PRN 17 Period
(e) PRN 24 ROTI
(j) PRN 17 ROTI
(k) IMF Bz
(b) PRN 28 DTEC
(g) PRN 15 DTEC
(c) PRN 28 Frequency
(h) PRN 15 Frequency
(d) PRN 28 Period
(i) PRN 15 Period
(e) PRN 28 ROTI
(j) PRN 15 ROTI
(b) PRN 16 DTEC
(g) PRN 10 DTEC
(c) PRN 16 Frequency
(h) PRN 10 Frequency
(d) PRN 16 Period
(i) PRN 10 Period
(e) PRN 16 ROTI
(j) PRN 10 ROTI
(b) PRN 2 DTEC
(g) PRN 27 DTEC
(c) PRN 2 Frequency
(h) PRN 27 Frequency
(d) PRN 2 Period
(i) PRN 27 Period
(e) PRN 2 ROTI
(j) PRN 27 ROTI
nT
TECu
Frequency (mHz)
Period (mins)
Magnitude
LT

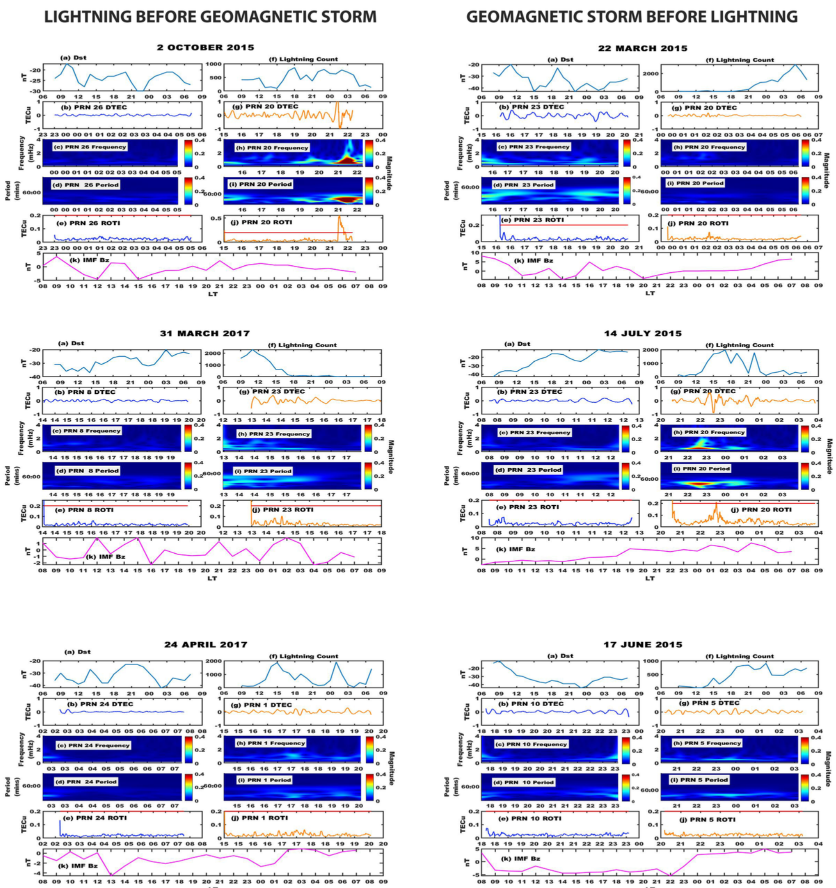
LIGHTNING BEFORE GEOMAGNETIC STORM
GEOMAGNETIC STORM BEFORE LIGHTNING
2 OCTOBER 2015
22 MARCH 2015
31 MARCH 2017
14 JULY 2015
24 APRIL 2017
17 JUNE 2015
(a) Dst
(f) Lightning Count
(b) PRN 26 DTEC
(g) PRN 20 DTEC
(c) PRN 26 Frequency
(h) PRN 20 Frequency
(d) PRN 26 Period
(i) PRN 20 Period
(e) PRN 26 ROTI
(j) PRN 20 ROTI
(k) IMF Bz
nT
TECu
Frequency (mHz)
Period (mins)
Magnitude
LT

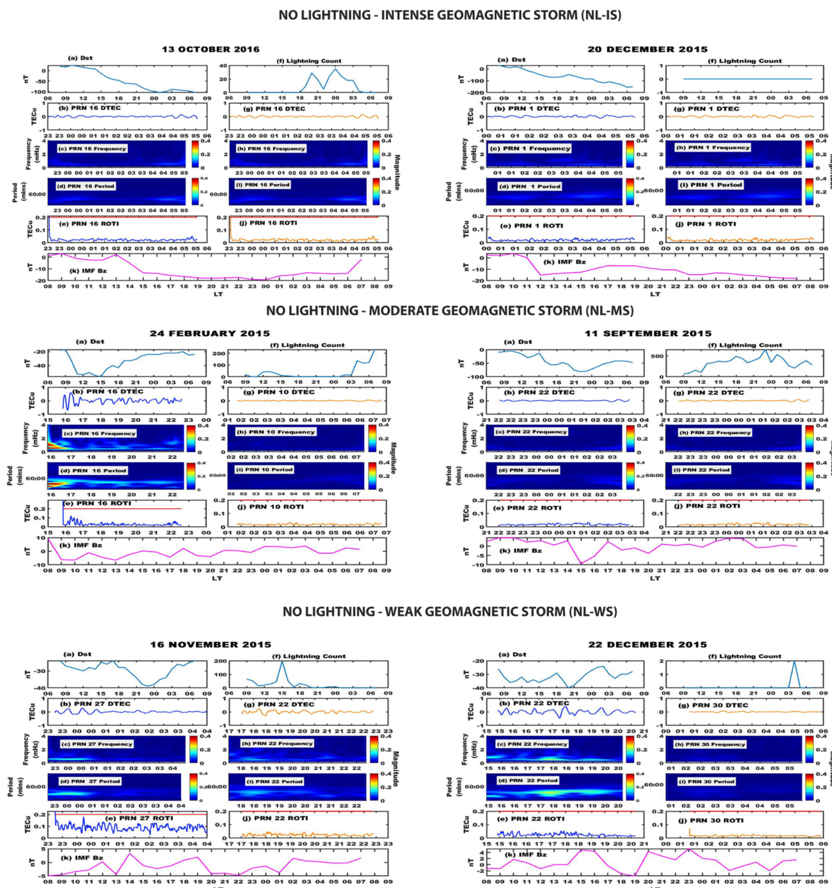
NO LIGHTNING - INTENSE GEOMAGNETIC STORM (NL-IS)
13 OCTOBER 2016
20 DECEMBER 2015
NO LIGHTNING - MODERATE GEOMAGNETIC STORM (NL-MS)
24 FEBRUARY 2015
11 SEPTEMBER 2015
NO LIGHTNING - WEAK GEOMAGNETIC STORM (NL-WS)
16 NOVEMBER 2015
22 DECEMBER 2015

Ionosphere Response to the simultaneous and consecutive occurrence of Geomagnetic Storm and Lightning at various intensities in a Low Latitude Region

Louis Osei-Poku[1,2], Wu Chen[1,2,*], Mingli Chen[3] ,Long Tang[4] and Akwasi Afrifa Acheampong[5]

[1] Department of Land Surveying and Geo-Informatics, The Hong Kong Polytechnic University, Kowloon, Hong Kong; louis.oseipoku@connect.polyu.hk, wu.chen@polyu.edu.hk
[2] Research Institute of Land and Space, The Hong Kong Polytechnic University, Kowloon, Hong Kong.
[3]Department of Building Environment and Energy Engineering, The Hong Kong Polytechnic University, Kowloon, Hong Kong; mingli.chen@polyu.edu.hk
[4] School of Civil and Transportation Engineering, Guangdong University of Technology, Guangzhou, China; ltang@gdut.edu.cn
[5] Department of Geomatic Engineering, Kwame Nkrumah University of Science and Technology, Kumasi, Ghana; aaacheampong.coe@knust.edu.gh

*Corresponding author: Wu Chen (wu.chen@polyu.edu.hk)

Key Points:

- Ionosphere response to geomagnetic storm or lightning occurring alone is non-different from when they occur simultaneously or consecutively
- The magnitude of the frequency of a disturbed ionosphere from lightning is 0.3-0.4
- The magnitude of frequency of a disturbed ionosphere from geomagnetic storm is 0.15-0.3

Abstract

Information from total electron content (TEC) from Global Navigation Satellite Systems (GNSS) could be assessed to know the impact of weather events to help in developing prediction and warning systems. Most studies focus on the occurrence of only one event neglecting situations where these weather events happen almost simultaneously or consecutively. This current study tends to fill the gap by analyzing ionosphere response following the simultaneous and/or consecutive occurrence of geomagnetic storm and lightning events at various intensities in southern China coastal region. The results showed that the magnitude of the frequency lightning-related events using continuous wavelet transform (CWT) was 0.3-0.4 while that of geomagnetic storm was 0.15-0.3. However, the various levels of intensity could not be distinguished. Being able to differentiate the weather events by the magnitude values following the ionosphere response is good for prediction and modeling purposes as the use of TEC in some studies does not provide this clear distinction.

Plain Language Summary

The atmosphere is subject to frequent weather activities like thunderstorms, geomagnetic storms, and typhoons. These activities at times do not only disrupt human lives directly such as death but also the telecommunication and navigation services on which we depend. In this study, we took a step further to identify how the atmosphere behaves when thunderstorms and geomagnetic storms happen at the same time or consecutively. Our results showed that thunderstorms will generate a magnitude of 0.3-0.4 while geomagnetic storms generated a magnitude of 0.15-0.3. The results are useful to improve upon the available weather prediction and modeling systems.

1 Introduction

The understanding of the interaction between space events, both natural and man-made, and the various layers of the atmosphere are essential in atmosphere science studies. The influx of energy and stream of particles from these events contribute to the magnetosphere-ionosphere-thermosphere coupling (MITC). The MITC could affect the total electron content (TEC) leading to amplitude and phase changes of radio signals of navigation and communication systems, disrupt power grid lines and cause blackouts (Adhikari et al., 2017). Phenomena or sources contributing to MITC could be external (outside the earth's atmosphere) or internal (on/near the earth's surface to about 500km upwards).

Geomagnetic storms are widely known external sources of influence to the MITC through the deposition of energy from field aligned current (FAC), ring current and auroral electrojets (McGranaghan et al., 2017). Several studies in the past decades on geomagnetic storm have been conducted to help understand its contribution to MITC. For instance, Ding et al. (2007) investigated travelling ionosphere disturbance (TID) propagation during the geomagnetic storm in October 2003 in the US Plains. They associated the cause of the TID with auroral westward electrojet. Cherniak and Zakharenkova (2018) attributed origin of TID to increase in magnitude of FAC and passage of solar terminator in the high latitude regions of Europe. Changes in TEC and global navigation satellite systems (GNSS) positioning errors were observed during the occurrence of geomagnetic storms. The internal sources contributing to MITC could be cyclones, earthquakes, volcanoes, and lightning. Yu and Liu (2021) and Chen et al. (2020) report on ionospheric condition and GNSS performance at the time of the passage of Tropical Cyclones Usagi and Manghkut respectively. Kong et al. (2018) studied the co-seismic ionosphere disturbance (CID) for the 2015 Nepal earthquake and ionosphere response to thunderstorms have been done by Ogunsua et al. (2020), Tang et al. (2019) ,Liu et al. (2021), Lay (2018) and Amin (2015).

Recently, most studies on these external and internal sources contributing to MITC are carried out using GNSS because of its wide spatio-temporal capabilities. The adverse effects resulting from these sources have rather become useful means by which GNSS could be deployed to investigate them. A comprehensive review of how GNSS has been deployed to study these sources (mostly weather events) can be found in Afraimovich et al. (2013). Despite the detailed use of GNSS to study these weather events, most studies done are weather-event-specific. That is, the occurrence of only one event at a particular instance is studied primarily to avoid influences of other events. Nonetheless, in real life situations, simultaneous and consecutive occurrence of these weather events are quite common and cannot be overlooked. This current study tends to add to the GNSS-weather event studies by observing the ionosphere response to simultaneous and consecutive occurrence of geomagnetic storm and lightning events in the low latitude of southern China coastal region. The data and methods are presented in Section 2. The results are presented and discussed in relation to other works in Sections 3 and 4 respectively. Conclusions and findings are summarized in Section 5.

2 Data and Methods

2.1 Lightning Data

The network consists of about 17 Vaisala LS8000 sensors which provide geolocation and source peak current of lightning in the area (Qin et al., 2020). The data spans from 2014 to 2017. A day with lightning count greater than 10,000 is deemed as "lightning day." (Osei-Poku et al., 2021). Different intensities of lighting are categorized as follows; Non-lightning (NL): count < 10,000, Moderate Lightning (ML): 10,000 ≤ count < 20,000, Intense Lighting (IL): 20,000 ≤ count < 40,000 and Super Lightning (SL): count ≥ 40,000. Where count is the number of times lightning happened.

2.2 Geomagnetic Data

Geomagnetic storm data used in this study are those that occurred in the declining phase of the 24th solar cycle due to the time range of data availability of lightning. Also, the 24th solar cycle spanning from 2008 to 2018 recorded fewer magnetic storms, which mostly occurred at the declining phase of the cycle, compared to previous cycles (Patel et al., 2019). Geomagnetic storm index of Disturbance Storm Time (dst) at various intensities as catergorized by Loewe (1997) as follows was adapted. No Storm (NS): dst > -30nT, Weak Storm (WS): -50nT < dst ≤ -30nT, Moderate Storm (MS): -100nT < dst ≤ -50nT, Intense Storm (IS): -200nT < dst ≤ -100nT and Super storm (SS): dst ≤ -200nT. The Data Analysis Center for Geomagnetism and Space Magnetism, Kyoto University, operating WDC for Geomangetism, Kyoto provided the dst-index data (IAGA 2002-liike format) (http://wdc.kugi.kyoto-u.ac.jp/dstae/index.html, accessed on 14 June 2019).

2.3 GNSS Data

GNSS data from the Hong Kong Satellite Reference (HK SatRef) available at https://www.geodetic.gov.hk/en/rinex/downv.aspx, (accessed on 14 June 2019) was used to detect ionosphere response to simultaneous and consecutive occurrence of geomagnetic storm and lightning. Slant TEC (STEC) initially computed from the well-known geometry free linear combination of pseudo- and carrier-phase signals was converted to vertical TEC (VTEC) by applying a mapping function as seen in Equation(1), where Re is the earth's radius, θ is the elevation angle at the ionosphere pierce point (IPP) of the signal–receiver path, and h_i is the ionospheric single layer, approximated at 350 km

$$\mathrm{VTEC} = \sqrt{1 - \left(\frac{\mathrm{R_e}\cos\theta}{\mathrm{R_e} + \mathrm{h_i}}\right)^2} * \mathrm{STEC} \quad (1)$$

VTEC was then detrended using Savitzky–Golay order of 6 and window length 120mins (Osei-Poku et al., 2021) to get detrended TEC (DTEC), using Equation (2). DTEC served as the input for spectral analysis.

$$\mathrm{DTEC} = \mathrm{VTEC} - \mathrm{VTEC_{savitzky-golay}} \quad (2)$$

Again, rate of TEC index (ROTI) defined by Pi et al. (1997) as the square root of TEC variance was used to determine the ionosphere response. ROTI could be used as a proxy to scintillation (Yang & Liu, 2016). ROTI at five minutes intervals of rate of TEC (ROT) was computed according to Equation (3), where ROT and ROTI are in TEC Units (TECu: 1TECu = 10^{16} e/m^2) per minute and the notation $\langle\cdot\rangle$ is the averaging operation. 0.2TECu is set as the threshold for ROTI (Wu et al., 2021).

$$\mathrm{ROTI} = \sqrt{\langle \mathrm{ROT}^2 \rangle - \langle \mathrm{ROT} \rangle^2} \quad (3)$$

2.4 Spectral Analysis

Ionosphere response is also analysed in the spectral domain to gain more insight. This is done by applying continuous wavelet transform (CWT) with Morlet as mother wavelet to the

DTEC to get information about its spectral content and how it changes with time (Amin, 2015). CWT is good for mapping properties of non-stationary signals, offers a good time-frequency and can adequately represent physical quantities (Amin, 2015; Chane-Ming et al., 2000).

2.5 Data groupings

The data sets are grouped and further analyzed as follows. Firstly, the categories of intensities of lightning and geomagnetic storm listed in Sections 2.1 and 2.2 were paired with other each. The parings of Super Lightning, Intense Lightning, Moderate Lightning and No Lightning with the various intensities of geomagnetic storm are referred to as Case 1, Case 2, Case 3, and Case 4 respectively. Secondly, there is a subdivision of each paring into lightning occurring before geomagnetic storm, geomagnetic storm happening before lightning and the two occurring at the same time except for Case 4 and Super Lightning (SL), Intense Lightning (IL), and Moderate Lightning (ML) parings with No Storm. Thirdly, each subdivision is further divided into disturbance from lightning only, geomagnetic storm only, from both and no disturbance. Figure 1 is a flow diagram of the data groupings.

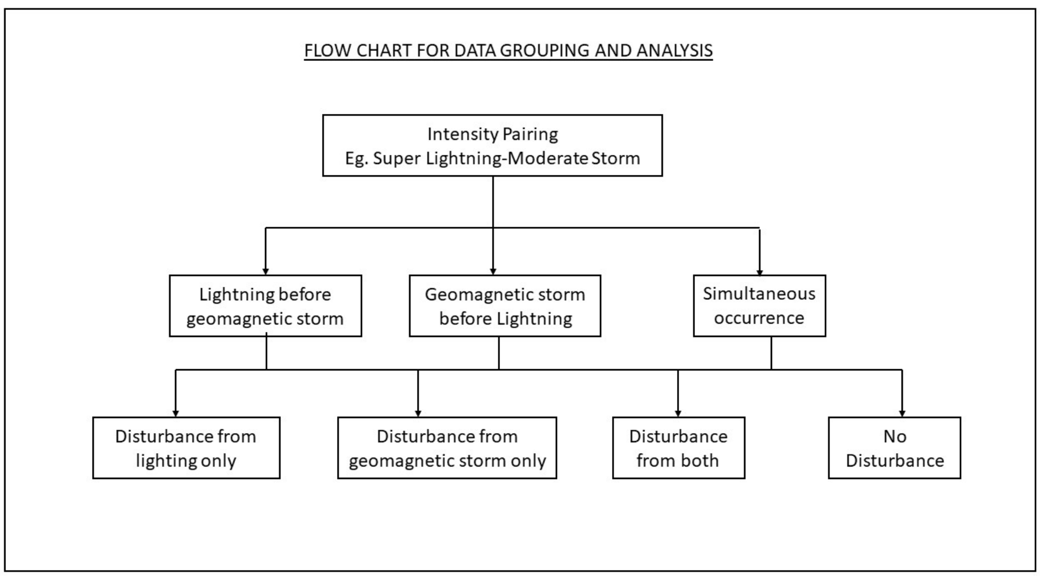

Figure 1. Flow Chart of the Data Groupings

3 Results

The results from this study based on the data sets are presented in this section. The number of days in each year under each intensity pairing is shown in Table 1.

Table 1 Number of days in each pairing

LEVEL OF INTENSITY PAIRINGS	Year	Super Geomagnetic Storm (SS)	Intense Geomagnetic Storm (IS)	Moderate Geomagnetic Storm (MS)	Weak Geomagnetic Storm (WS)	No Geomagnetic Storm (NS)
Super Lightning (SL) Case 1	2014	0	0	2	9	63
	2015	0	1	9	10	62
	2016	0	0	8	15	68
	2017	0	0	4	11	51
Intense Lightning (IL) Case 2	2014	0	0	1	3	0
	2015	1	0	4	5	11
	2016	0	0	3	6	0
	2017	0	0	2	4	0
Moderate Lightning (ML) Case 3	2014	0	0	0	0	14
	2015	0	1	4	8	8
	2016	0	0	5	2	14
	2017	0	0	0	7	27
No Lightning (NL) Case 4	2014	0	0	7	21	76
	2015	1	3	24	46	140
	2016	0	2	16	41	160
	2017	0	2	7	37	188

From Table 1, the intensities of lightning with that of moderate and weak storm had high number of days with the rest almost being null. Focus is then shifted to the pairings with high number of days. Table 2 to Table 4 show the number of days in each subdivision with their corresponding disturbances as according to the flow chart in Figure 1.

Table 2 Number of days of Storm before Lightning and the corresponding days of disturbances

LEVEL OF INTENSITY PAIRINGS	Year	Geomagnetic Storm before lightning	Disturbance from Geomagnetic Storm only	Disturbance from Lightning only	Disturbance from Both Lightning and Geomagnetic Storm	Without Disturbance from Both Lightning and Geomagnetic Storm
Super Lightning - Moderate Geomagnetic Storm (SL-MS) Case 1	2014	0	0	0	0	0
	2015	2	0	0	0	2
	2016	4	0	3	1	0
	2017	1	0	1	0	0
Intense Lightning - Moderate Geomagnetic Storm (IL-MS) Case 2	2014	5	0	1	0	4
	2015	6	1	1	1	3
	2016	6	0	3	0	3
	2017	8	1	3	2	2
Intense Lightning - Moderate Geomagnetic Storm (IL-MS) Case 2	2014	1	0	0	1	0
	2015	1	0	0	0	1
	2016	1	0	0	0	1
	2017	1	0	0	1	0
Intense Lightning - Weak Storm (IL-WS) Case 2	2014	3	1	1	0	1
	2015	2	0	2	0	0
	2016	1	0	0	0	1
	2017	3	0	0	0	3
Moderate Lightning - Moderate Geomagnetic Storm (ML-MS) Case 3	2014	-	-	-	-	-
	2015	2	0	1	0	1
	2016	1	0	0	0	1
	2017	-	-	-	-	-

Moderate Lightning - Weak Geomagnetic Storm (ML-WS) Case 3	2014	-	-	-	-	-
	2015	5	1	1	0	3
	2016	0	0	0	0	0
	2017	3	0	0	0	1

Table 3 Number of Days of Lightning before Storm and the corresponding days of disturbances

LEVEL OF INTENSITY PAIRINGS	Year	Lightning before Geomagnetic Storm	Disturbance from Lightning only	Disturbance from Geomagnetic Storm only	Disturbance from Both Lightning and Geomagnetic Storm	Without Disturbance from Both Lightning and Geomagnetic Storm
Super Lightning - Moderate Geomagnetic Storm (SL-MS) Case 1	2014	1	1	0	0	0
	2015	5	2	0	0	3
	2016	2	1	0	0	1
	2017	3	1	1	0	1
Intense Lightning - Moderate Geomagnetic Storm (IL-MS) Case 2	2014	4	1	0	0	3
	2015	4	2	0	0	2
	2016	9	3	0	1	5
	2017	3	2	0	0	1
Intense Lightning - Moderate Geomagnetic Storm (IL-MS) Case 2	2014	0	0	0	0	0
	2015	3	1	0	2	0
	2016	2	0	1	1	0
	2017	1	0	0	0	1
Intense Lightning - Weak Geomagnetic Storm (IL-WS) Case 2	2014	0	0	0	0	0
	2015	2	0	1	0	1
	2016	4	1	0	2	1
	2017	1	0	1	0	0
Moderate Lightning - Moderate Geomagnetic Storm (ML-MS) Case 3	2014	-	-	-	-	-
	2015	2	2	0	0	0
	2016	4	1	0	0	3
	2017	-	-	-	-	-

Moderate Lightning - Weak Geomagnetic Storm (ML-WS) Case 3	2014	-	-	-	-	-
	2015	2	1	0	0	1
	2016	2	1	0	0	1
	2017	3	0	0	1	2

Table 4 Number of days of Lightning and Storm happening at the same time and the corresponding days of disturbances

LEVEL OF INTENSITY PAIRINGS	Year	Lightning and Geomagnetic Storm at the same time	Disturbance from Lightning only	Disturbance from Geomagnetic Storm only	Disturbance from Both Lightning and Geomagnetic Storm	Without Disturbance Both Lightning and Geomagnetic Storm
Super Lightning - Moderate Geomagnetic Storm (SL-MS) Case 1	2014	1	0	0	1	0
	2015	1	0	0	0	1
	2016	2	2	0	0	0
	2017	0	0	0	0	0
Intense Lightning - Moderate Geomagnetic Storm (IL-MS) Case 2	2014	0	0	0	0	0
	2015	0	0	0	0	0
	2016	0	0	0	0	0
	2017	0	0	0	0	0
Intense Lightning - Moderate Geomagnetic Storm (IL-MS) Case 2	2014	0	0	0	0	0
	2015	0	0	0	0	0
	2016	0	0	0	0	0
	2017	0	0	0	0	0
Intense Lightning - Weak Geomagnetic Storm (IL-WS) Case 2	2014	0	0	0	0	0
	2015	1	0	0	0	1
	2016	1	0	0	1	0
	2017	0	0	0	0	0
Moderate Lightning - Moderate Geomagnetic Storm (ML-MS)	2014	-	-	-	-	-
	2015	0	0	0	0	0
	2016	0	0	0	0	0
	2017	-	-	-	-	-

Case 3						
Moderate Lightning - Weak Geomagnetic Storm (ML-WS) Case 3	2014	-	-	-	-	-
	2015	1	0	0	0	1
	2016	0	0	0	0	0
	2017	1	0	0	0	1

Further to Table 2 to Table 4, it could be seen that storm and lightning happening at the same time was mostly null. Hence this subdivision is ignored. Focus is now shifted to the subdivisions of lightning before storm and vice versa. From the days in these subdivisions and their corresponding disturbances all the years have similar pattern for the number of days. Individual days are therefore selected to represent the intensity paring's subdivision, and their corresponding disturbances.

To indicate the ionosphere response to lightning and geomagnetic storm, time domain of DTEC, period and frequency of DTEC obtained using CWT, and the ROTI of available satellites or pseudorandom noise codes (PRN) are shown. An average of six GPS PRNs are available at any given time and the stations of HK Satref are quite close; hence the observations on the PRNs by the stations tend to have similar characteristics (Tang et al., 2019). Therefore, only one PRN from one station is presented. The PRNs available at about the exact time of the minimum dst for the magnetic storm days are chosen as magnetic storm usually make an immediate impact on the ionosphere (Borries et al., 2009; Ding et al., 2007). According to Osei-Poku, Tang, Chen, Chen and Acheampong (2022) , lightning dominant in daytime in the study area see some hours delay while those dominant in the nighttime have a relative instant impact on the ionosphere. The period where lightning is dominant was checked and the available PRN at the expected time of ionosphere disturbance was selected.

The days under an intensity pairing are placed together as one figure. All the panels for the individual days follow the same arrangement. The top row panels (a and f) show the dst and lightning count. The second to fifth row panels (b, g, c, h, d, and i) show DTEC in time domain, DTEC in frequency domain, period, and ROTI of the PRN respectively. The bottom row panel (k) shows the Bz component of the interplanetary magnetic field (IMF). The x-axis of the figure panels is in hours of local time (LT: UT+8). The presentation of the figures of the individual days is based on the chronological ascension order of Cases stated in Section 2.3 above.

3.1 Case 1 (Super Lightning pairings)

3.1.1 Super Lightning – Moderate Geomagnetic Storm (SL-MS) pairings

The days of intensity pairing SL-MS and its subdivisions using the flow chart in Figure 1 are shown in Figure 2. Days of subdivision related to Lightning are on the left column while that of geomagnetic storm are on the right column. The individual subdivisions are further elaborated as follows:

3.1.1.1 Lightning before Geomagnetic Storm with disturbance from lightning only under Super Lightning-Moderate Geomagnetic Storm (SL-MS) pairing.

4th July 2015 was the day for this subdivision and occupies the top left corner of Figure 2. Dst was increasing steadily from 0 to 20nT from the beginning of the day till 23LT. After 00LT, it decreases to -20nT at 03LT, becomes stable for a while and further decreases to its minimum of -58nT at 05LT as seen panel a of **Error! Reference source not found.**. IMF Bz in panel k also recorded its minimum value around the same time of dst. PRN 25 was available at the time of the minimum of dst. As can be seen in panel b of this day, there were DTEC changes about the same time dst was minimum. Frequency of 0.1mHz and period of 37 mins were recorded at the same time (panels c-d). Nonetheless, the ROTI in panel e could not exceed the threshold of 0.2. Lightning as seen in panel f was dominant in the evening around 18-21LT. The expected ionosphere disturbance is about the same time as its peak. DTEC of PRN 5 in panel g of **Error! Reference source not found.** shows changes at 19-21LT. The DTEC has a frequency of 0.67mHz and period of 25 mins. PRN 5 had ROTI exceeding the threshold indicating a disturbance.

3.1.1.2 Lightning before Geomagnetic Storm with disturbance from storm only under Super Lightning-Moderate Geomagnetic Storm (SL-MS) pairing.

16th July 2017 was the day for this subdivision and occupies the second row under lightning before geomagnetic storm column of Figure 2. The minimum dst of -72nT occurred at 23LT as seen in panel a of this day. IMF Bz in panel k also recorded its minimum value around the same time. PRN 5 was available with DTEC changes about the same time of minimum dst with frequency of 0.9mHz, amplitude of 0.5, a period of 19 mins and ROTI exceeding the threshold of 0.2. Lightning as seen in panel f was dominant around 15-17LT. The ionosphere response is expected around 17-19LT. PRN 17 was available around 17-19LT recording frequency of 0.8mHz, amplitude of 0.08, period of 20 mins but ROTI not exceeding the threshold.

3.1.1.3 Lightning before Geomagnetic Storm with no disturbance from both events under Super Lightning-Moderate Geomagnetic Storm (SL-MS) pairing.

The day for this subdivision was 15th August 2015 which occupies the bottom left corner of Figure 2. The minimum dst of -57nT occurred at 03LT as seen in panel a of this day. IMF Bz in panel k also recorded its minimum value around the same time. PRN 22 was available with DTEC changes about the same time of minimum dst with frequency of 0.8mHz, amplitude of 0.1, a period of 20 mins. Lightning as seen in panel f was dominant around 09-11LT. The ionosphere response is expected to be around 12-15LT. PRN 1 was available recording frequency of 0.8mHz, amplitude of 0.06 and period of 20 mins. ROTI did not exceed the threshold for both events.

3.1.1.4 Geomagnetic Storm before Lightning with disturbance from lightning only under Super Lightning-Moderate Geomagnetic Storm (SL-MS) pairing.

The day for this subdivision was 17th March 2016 which occupies the top right corner of Figure 2. The minimum dst of -52nT occurred at 12LT as seen in panel a. IMF Bz in panel k also recorded its minimum value around 10LT. Frequency of 0.9mHz, amplitude of 0.06, and a period of 20 mins was recorded by PRN 32 which was available about the same time of minimum dst. Lightning as seen in panel f was dominant around 18-20LT. The ionosphere response is expected about same time. PRN 17 was available recording frequency of 1.1mHz, amplitude of 0.12 and period of 18 mins. ROTI exceeded the threshold for only lightning.

3.1.1.5 Storm before Lightning with disturbance from both under Super Lightning-Moderate Storm (SL-MS) pairing.

The day for this subdivision was 1st September 2016 which occupies the middle row of the right column of Figure 2. The minimum dst of -59nT occurred at 17LT just an hour before lightning peak at 18LT as seen in panels a and b of **Error! Reference source not found.**. The ionosphere response was expected at 17-20LT for both events. PRN 21 was available at this time hence could be assessed. The frequency of 0.8mHz, amplitude of 0.1, and a period of 20 mins was recorded. ROTI exceeded the threshold.

3.1.1.6 Storm before Lightning with no disturbance from events under Super Lightning-Moderate Storm (SL-MS) pairing.

23rd July 2016 is the day for this subdivision which occupies the bottom right corner of Figure 2. The minimum dst of -63nT occurred at 15LT as seen in panel a. IMF Bz in panel k also recorded its minimum value around 12-15LT. The available PRN, 1, recorded a frequency of 0.6mHz, amplitude of 0.03, and a period of 27 mins. Lightning as seen in panel f was dominant most around 04-06LT. The available PRN, 25 recorded a frequency of 1.4mHz, amplitude of 0.004 and period of 16 mins. ROTI did not exceed the threshold for both.

3.1.2 Super Lightning – Weak Geomagnetic Storm (SL-WS) pairings

The days of intensity pairing SL-WS and its subdivisions using the flow chart in Figure 1 are shown in Figure 3. Days of subdivision related to Lightning are on the left column while that of geomagnetic storm are on the right column. The individual subdivisions are further elaborated as follows:

3.1.2.1 Lightning before Geomagnetic Storm with disturbance from lightning only under Super Lightning-Weak Geomagnetic Storm (SL-WS) pairing.

18th May 2015 is the day for this subdivision which occupies the top left corner of Figure 3. The minimum dst of -42nT occurred at 07LT as seen in panel a of this day. IMF Bz in panel k also recorded its minimum at the same time. The available PRN, 13, recorded a frequency of

0.7mHz, amplitude of 0.01, and a period of 24 mins. Lightning as seen in panel f was dominant around 18-21 LT. The available PRN 10 also recorded a frequency of 0.7mHz and period of 24 mins but amplitude of 0.35 with ROTI exceeding the threshold.

3.1.2.2 Lightning before Geomagnetic Storm with disturbance from both events under Super Lightning-Weak Geomagnetic Storm (SL-WS) pairing.

8th September 2016 is the day for this subdivision which occupies the second row of the left column of Figure 3. The minimum dst of -33nT occurred at 18LT as seen in panel a of this day. IMF Bz in panel k also recorded its minimum at the same time. Lightning as seen in panel f was dominant around 15-17 LT. PRN 24 recorded a frequency of 0.6mHz, amplitude of 0.14, and a period of 27 mins during the time of the storm while PRN 15 recorded a frequency of 1.1mHz, amplitude of 0.13, and a period of 15 mins at the time of lightning. Both had ROTI exceeding the threshold.

3.1.2.3 Lightning before Geomagnetic Storm with no disturbance from both events under Super Lightning-Weak Geomagnetic Storm (SL-WS) pairing.

6th June 2016 is the day for this subdivision which occupies the third row of the left column of Figure 3. Minimum dst was -44nT happening at 14LT as seen in panel a. A frequency of 0.7mHz, amplitude of 0.08, and a period of 24 mins was observed on PRN 11 at 14LT. Lightning as seen in panel f was dominant around 09LT. The available PRN 27 recorded a frequency of 0.9mHz, amplitude of 0.08 and period of 18 mins. ROTI did not exceed the threshold for both PRNs.

3.1.2.4 Geomagnetic Storm before Lightning with disturbance from storm only under Super Lightning-Weak Geomagnetic Storm (SL-WS) pairing.

14th May 2015 is the day for this subdivision which occupies the top right corner of Figure 3. Minimum dst was -33nT happening at 13LT as seen in panel a of this day. A frequency of 1.2mHz, amplitude of 0.17, and a period of 13 mins was observed on PRN 19 at 13LT with ROTI exceeding the threshold. Lightning as seen in panel f was dominant around 16LT. The available PRN 4 recorded a frequency of 0.9mHz, amplitude of 0.09 and period of 18 mins.

3.1.2.5 Geomagnetic Storm before Lightning with disturbance from lightning only under Super Lightning-Weak Geomagnetic Storm (SL-WS) pairing

The day for this subdivision is 11th June 2015 and it is seen at the second row of the right column of Figure 3. Minimum dst was -33nT happening at 11LT as seen in panel a of **Error! Reference source not found.**. A frequency of 1.3mHz, amplitude of 0.09, and a period of 12 mins was observed on PRN 16 at 11LT. Lightning as seen in panel f was dominant around 16LT. The available PRN 5 recorded a frequency of 0.9mHz, amplitude of 0.6 and period of 18 mins with ROTI exceeding the threshold.

3.1.2.6 Geomagnetic Storm before Lightning with disturbance from both events under Super Lightning-Weak Geomagnetic Storm (SL-WS) pairing

The day for this subdivision is 19th May 2015 which can be seen in the third row of the right column of Figure 3. The minimum dst was -44nT happening at 11LT as seen in panel a of this day. PRN 19 available at 11LT recorded a frequency of 1mHz, amplitude of 0.2, and a period of 16 mins. Lightning as seen in panel f was dominant around 15-18LT. The available PRN 17 recorded a frequency of 0.9mHz, amplitude of 0.45 and period of 18 mins. ROTI exceeded the threshold for both events.

3.1.2.7 Geomagnetic Storm before Lightning with no disturbance from both events under Super Lightning-Weak Geomagnetic Storm (SL-WS) pairing

The day for this subdivision is 10th June 2015 which can be seen in the bottom right corner of Figure 3. The minimum dst was -31nT at 08LT as seen in panel a of this day. PRN 16 available at 08LT recorded a frequency of 1mHz, amplitude of 0.1, and a period of 16 mins. Lightning as seen in panel f was dominant around 15-18LT. The available PRN 2 also recorded a frequency of 1mHz, amplitude of 0.1 and period of 16 mins. ROTI did not exceed the threshold for both events.

3.1.3 Super Lightning – No Geomagnetic Storm (SL-NS) pairings

The days of intensity pairing SL-NS and its subdivisions using the flow chart in Figure 1 are shown in the top row of Figure 4. The individual subdivisions are further elaborated as follows:

3.1.3.1 Super Lightning-No Geomagnetic Storm (SL-NS) pairing with disturbance from lightning.

29th April 2015 is the day for this subdivision which can be seen in the top left corner of Figure 4. There was no storm as minimum dst was -16nT happening at 06LT as seen in panel a of **Error! Reference source not found.**. The available PRN, 20, recorded a frequency of 0.9mHz, amplitude of 0.02, and a period of 18 mins. Lightning as seen in panel f was most dominant around 18-22LT. The available PRN, 10 recorded a frequency of 0.5mHz, amplitude of 0.25 and period of 33 mins with ROTI exceeding the threshold.

3.1.3.2 Super Lightning-No Geomagnetic Storm (SL-NS) pairing with no disturbance.

21st May 2015 is the day for this subdivision which can be seen in the top right corner of Figure 4. There was no storm as minimum dst was -18nT happening at 08LT as seen in panel a of this day. A frequency of 0.8mHz, amplitude of 0.08, and a period of 20 mins was observed on

PRN 20 available at 08LT. Lightning as seen in panel f was dominant most around 12-15LT. The available PRN, 19 recorded a frequency of 0.6mHz, amplitude of 0.15 and period of 27 mins with ROTI not exceeding the threshold.

3.2 Case 2 (Intense lightning pairings)

3.2.1 Intense Lightning – Moderate Geomagnetic Storm (IL-MS) pairings

The days of intensity pairing IL-MS and its subdivisions using the flow chart in Figure 1 are shown Figure 5. The individual subdivisions are further elaborated as follows:

3.2.1.1 Lightning before Geomagnetic Storm with disturbance from storm only under IL-MS pairing

13th April 2016 is the day for this subdivision which can be seen in the top left corner of Figure 5. Minimum dst was -55nT which occurred at 13LT as seen in panel a of this day. A frequency of 1.1mHz, amplitude of 0.15, and a period of 15 mins was observed on PRN 8 at 13LT. Lightning as seen in panel f was dominant around 09LT. The available PRN 16 recorded a frequency of 0.7mHz, amplitude of 0.08 and period of 23mins.

3.2.1.2 Lightning before Geomagnetic Storm with disturbance from both under IL-MS pairing

The day for this subdivision was 8th June 2015 which can be seen in the middle row of the first column of Figure 5. The minimum dst of -73nT occurred at 17LT few hours after lightning peak at 13LT as seen in its panels a and b. The ionosphere response was expected at 17-20LT for both events. PRN 6 was available at this time hence could be assessed. The frequency of 0.6mHz, amplitude of 0.25, and a period of 27 mins was recorded. ROTI exceeded the threshold.

3.2.1.3 Lightning before Geomagnetic Storm with no disturbance from both under IL-MS pairing

The day for this subdivision is 17th July 2017 which can be seen in the bottom left corner of Figure 5. The minimum dst was -61nT at 00LT as seen in panel a of this day. PRN 24 available at 00LT recorded a frequency of 0.8mHz, amplitude of 0.02, and a period of 21 mins. Lightning as seen in panel f was dominant around 15-18LT. The available PRN 2 also recorded the same values of frequency, amplitude, and period like PRN 24. ROTI did not exceed the threshold for both events.

3.2.1.4 Geomagnetic Storm before Lightning with disturbance from both under IL-MS pairing

28th September 2017 was the day for this subdivision which occupies the top right corner of Figure 5. The minimum dst was -55nT at 14LT as seen in panel a of this day. PRN 15 available at 00LT recorded a frequency of 1.1mHz, amplitude of 0.25, and a period of 15 mins. Lightning as seen in panel f was dominant around 16-18LT. The available PRN 24 recorded frequency of 1.2mHz, amplitude of 0.3, and period 13 of mins. ROTI exceeded the threshold for both events.

3.2.1.5 Geomagnetic Storm before Lightning with no disturbance from both under IL-MS pairing

8th May 2016 was the day for this subdivision which is seen in the middle row of the right column of Figure 5. The minimum dst was -88nT at 16LT as seen in panel a of this day. PRN 1 available at 16LT recorded a frequency of 0.5mHz, amplitude of 0.09, and a period of 32 mins. Lightning as seen in panel f was dominant around 16-18LT. The available PRN 24 recorded frequency of 1.2mHz, amplitude of 0.04, and period 13 of mins. ROTI did not exceed the threshold for both events.

3.2.2 Intense Lightning – Weak Geomagnetic Storm (IL-WS) pairings

The days of intensity pairing IL-WS and its subdivisions using the flow chart in Figure 1 are shown Figure 6. The individual subdivisions are further elaborated as follows:

3.2.2.1 Lightning before Geomagnetic Storm with disturbance from lightning only under IL-WS

26th July is the day for this subdivision which is seen at the top left corner of Figure 6. Minimum dst was -36nT which occurred at 08LT as seen in panel a of this day. A frequency of 0.9mHz, amplitude of 0.02, and a period of 18 mins was observed on PRN 4 at 08LT. Lightning as seen in panel f was dominant around 16LT. The available PRN 20 also recorded a frequency of 0.9mHz, and period of 18 mins but amplitude of 0.18.

3.2.2.2 Lightning before Geomagnetic Storm with disturbance from storm only under IL-WS

The day for this subdivision is 15th June 2015 which occupies the middle row of the left column of Figure 6. Minimum dst was -34nT happening at 00LT as seen in its panel a. A frequency of 0.6mHz, amplitude of 0.45, and a period of 27 mins was observed on PRN 5 at 00LT. Lightning as seen in panel f was dominant around 16LT. The available PRN 17 also recorded a frequency of 0.6mHz, and period of 18 mins but amplitude of 0.1.

3.2.2.3 Lightning before Geomagnetic Storm with no disturbance from both events under IL-WS

The day for this subdivision is 5th September 2016 which can be seen at the bottom left corner of Figure 6. Minimum dst was -38nT happening at 03LT as seen in panel a this day. A frequency of 1mHz, amplitude of 0.01, and a period of 16 mins was observed on PRN 26 at 03LT. Lightning as seen in panel f was dominant around 19LT. The available PRN 24 recorded a frequency of 0.6mHz, amplitude of 0.07, and period of 27 mins.

3.2.2.4 Geomagnetic Storm before Lightning with disturbance from storm only under IL-WS

The day for this subdivision is 21st August 2014. It can be seen at the top right corner of Figure 6. The minimum dst was -30nT happening at 15LT as seen in its panel a. A frequency of 0.9mHz, amplitude of 0.4, and a period of 18 mins was observed on PRN 2 at 15LT. Lightning as seen in panel f was dominant around 17LT. The available PRN 26 recorded a frequency of 0.8mHz, amplitude of 0.07, and period of 20 mins.

3.2.2.5 Geomagnetic Storm before Lightning with disturbance from lightning only under IL-WS pairing

The day for this subdivision is 14th September 2014 which can be seen at the middle row of the right column of Figure 6. The minimum dst was -40nT happening at 09LT as seen in panel a of this day. A frequency of 0.9mHz, amplitude of 0.05, and a period of 18 mins was observed on PRN 28 at 09LT. Lightning as seen in panel f was dominant around 17LT. The available PRN 5 also recorded the same frequency and period like PRN 28 but amplitude of 0.38 with ROTI exceeding the threshold.

3.2.2.6 Geomagnetic Storm before Lightning with no disturbance from both events under IL-WS pairing

The day for this subdivision is 19th September 2014 which can be seen at the bottom right corner of Figure 6. Minimum dst was -40nT happening at 12LT as seen in panel a this day. A frequency of 0.6mHz, amplitude of 0.1, and a period of 27 mins was observed on PRN 28 at 09LT. Lightning as seen in panel f was dominant around 17LT. The available PRN 18 also recorded a frequency of 1mHz, amplitude of 0.1, and a period of 18 mins. ROTI did not exceed the threshold.

3.2.3 Intense Lightning – No Geomagnetic Storm (IL-NS) pairings

The days of intensity pairing IL-NS and its subdivisions using the flow chart in Figure 1 are shown in the middle row of Figure 4. The individual subdivisions are further elaborated as follows:

3.2.3.1 Intense Lightning-No Geomagnetic Storm (IL-NS) pairing with disturbance from lightning.

1st May 2015 is the day for this subdivision which can be seen at the middle row of the first column of Figure 4. There was no storm as minimum dst was -6nT which happened at 13LT as seen in panel a of this day. The available PRN, 27, recorded a frequency of 0.9mHz, amplitude of 0.1, and a period of 18 mins. Lightning as seen in panel f was dominant most around 17LT. The available PRN 28 also recorded a frequency of 0.9mHz, period of 18 mins but amplitude of 0.3 with ROTI exceeding the threshold.

3.2.3.2 Intense Lightning-No Storm (IL-NS) pairing with no disturbance

3rd September 2015 is the day for this subdivision which can be seen at the middle row of the second column of Figure 4. There was no storm as minimum dst was -13nT which happened at 14LT as seen in its panel a. Lightning as seen in panel f was dominant most around 13LT. PRN 6 was available at these times hence could be accessed for both events. It recorded a frequency of 0.9mHz, a period of 18 mins and amplitude of 0.09-0.1 for both events.

3.3 Case 3 (Moderate lightning pairings)

3.3.1 Moderate Lightning – Moderate Geomagnetic Storm (ML-MS) pairings

The days of intensity pairing ML-MS and its subdivisions using the flow chart in Figure 1 are shown in Figure 7. The individual subdivisions are further elaborated.

3.3.1.1 Lightning before Geomagnetic Storm with disturbance from lightning only under ML-MS

The day for this subdivision is 25th June 2015 which can be seen at the top left corner of Figure 7. The minimum dst was -86nT which occurred at 21-00LT as seen in panel a of this day. A frequency of 1.1mHz, amplitude of 0.07, and a period of 15 mins was observed on PRN 24 around this time. Lightning as seen in panel f was dominant around 15LT. The available PRN 17 recorded a frequency of 0.7mHz, amplitude of 0.3 and period of 23mins.

3.3.1.2 Lightning before Geomagnetic Storm with no disturbance from both under ML-MS pairing

The day for this subdivision is 25th October 2015 which occupies the bottom left corner of Figure 7. The minimum dst was -59nT which occurred at 01LT as seen in its panel a. A frequency of 0.7mHz, amplitude of 0.06, and a period of 23 mins was observed on PRN 16 around this time. Lightning as seen in panel f was dominant around 18LT. The available PRN 10 recorded a frequency of 0.5mHz, amplitude of 0.1 and period of 32mins.

3.3.1.3 Geomagnetic Storm before Lightning with disturbance from lightning only under ML-MS pairing

8th September 2015 is the day for this subdivision which occupies the top right corner of Figure 7. Minimum dst was -66nT which occurred at 10LT as seen in panel a of this day. Lightning as seen in panel f was dominant around 17LT. PRN 28 and 15 recorded a frequency of 0.5mHz, a period of 32 mins but amplitudes of 0.09 and 0.13 for storm and lightning respectively

3.3.1.4 Geomagnetic Storm before Lightning with no disturbance from both under ML-MS pairing

29th September 2016 is the day for this subdivision which is seen at the bottom left corner of Figure 7. Minimum dst was -66nT which occurred at 17LT as seen in panel a of this day. Lightning as seen in panel f was dominant around 03-06LT. PRN 2 and 27 recorded a frequency of 0.6mHz, a period of 27 mins but amplitudes of 0.11 and 0.06 for geomagnetic storm and lightning respectively.

3.3.2 Moderate Lightning – Weak Geomagnetic Storm (ML-WS) pairings

The days of intensity pairing ML-MS and its subdivisions using the flow chart in Figure 1 are shown in Figure 8. The individual subdivisions are further elaborated.

3.3.2.1 Lightning before Geomagnetic Storm with disturbance from lightning only under ML-WS pairing

2nd October 2015 is the day for this subdivision which can be seen at the top left corner of Figure 8. Minimum dst was -30nT which occurred at 23LT as seen in panel a of this day. Lightning as seen in panel f was dominant around 21LT. PRN 26 and 20 recorded a frequency of 0.7mHz, a period of 23 mins but amplitudes of 0.01 and 0.5 for storm and lightning respectively

3.3.2.2 Lightning before Geomagnetic Storm with disturbance from both under ML-WS pairing

The day for this subdivision is 31st March 2017 which can be seen at the middle row of the left column of Figure 8. Minimum dst was -37nT which occurred at 14LT as seen in its panel a. Lightning as seen in panel f was dominant around 11LT. PRN 8 recorded a frequency of 0.9mHz, a period of 18 mins and amplitude of 0.98 at the time of storm while PRN 23 recorded a frequency of 0.7mHz, amplitude of 0.1 and period of 23 mins at the time of lightning.

3.3.2.3 Lightning before Geomagnetic Storm with no disturbance from both under ML-WS pairing

The day for this subdivision is 24th April 2017 which occupies the bottom left corner of Figure 8. Minimum dst was -42nT which occurred at 02LT as seen in panel a. Lightning as seen in panel f was dominant most around 15LT. PRN 24 recorded a frequency of 0.9mHz, a period of 18 mins and amplitude of 0.08 at the time of storm while PRN 1 recorded a frequency of 1.2mHz, amplitude of 0.06 and period of 13 mins at the time of lightning.

3.3.2.4 Geomagnetic Storm before Lightning with disturbance from storm only under ML-WS pairing

The day for this subdivision is 22nd March 2015 which is seen at the top right corner of Figure 8. Minimum dst was -43nT which occurred at 15LT as seen in its panel a. Lightning as seen in panel f was dominant most around 05LT. PRN 23 and 20 recorded frequencies of 0.9mHz, period of 18 mins but amplitudes of 0.18 and 0.04 at the time of storm and lightning respectively.

3.3.2.5 Geomagnetic Storm before Lightning with disturbance from lightning only under ML-WS pairing

The day for this subdivision is 14th July 2015 which is seen at the middle row of the right column of Figure 8. Minimum dst was -43nT which occurred at 08LT as seen in its panel a. Lightning as seen in panel f was dominant most around 17LT. PRN 23 and 20 recorded frequencies of 0.9mHz, period of 18 mins but amplitudes of 0.04 and 0.45 at the time of storm and lightning respectively.

3.3.2.6 Geomagnetic Storm before Lightning with no disturbance from both under ML-WS pairing

17th June 2015 is the day for this subdivision which can be seen at the bottom left corner of Figure 8. Minimum dst was -44nT which occurred at 23LT as seen in panel a of this day. Lightning as seen in panel f was dominant most around 00LT. Both PRN 10 and 5 recorded frequencies of 0.7mHz, period of 23 mins and amplitudes of 0.09 at the time of storm and lightning respectively.

3.3.3 Moderate Lightning – No Geomagnetic Storm (ML-NS) pairings

The days of intensity pairing ML-NS and its subdivisions using the flow chart in Figure 1 are shown in the bottom row of Figure 4. The individual subdivisions are further elaborated.

3.3.3.1 Moderate Lightning-No Geomagnetic Storm (ML-NS) with disturbance from lightning

21st November 2015 is the day for this subdivision which can be seen at the bottom left corner of Figure 4. This day was magnetically quiet as the minimum dst was -15nT which occurred at 09LT as seen in its panel a. Lightning as seen in panel f was dominant most around 09LT. Both PRN 5 and 15 recorded frequencies of 0.8mHz, period of 20 mins but different amplitudes of 0.09 and 0.45 at the time of storm and lightning respectively. The high amplitudes on PRN 5 are seen at the expected time of lightning disturbance.

3.3.3.2 Moderate Lightning-No Geomagnetic Storm (ML-NS) with no disturbance

5th August 2016 is the day for this subdivision which can be seen at the bottom right corner of Figure 4. This day was magnetically quiet as minimum dst was -28nT which occurred at 16LT as seen in its panel a. Lightning as seen in panel f was dominant most around 16LT.

PRN 2 was available at this time hence could be accessed for both events. It recorded a frequency of 0.5mHz, a period of 32 mins and amplitude of 0.1 for both events.

3.4 Case 4 (No lightning pairings)

The days of intensity pairing NL and its subdivisions using the flow chart in Figure 1 are shown in Figure 9. The individual subdivisions are further elaborated.

3.4.1 No Lightning-Intense Geomagnetic Storm (NL-IS) with disturbance from storm

13th October 2016 was the day for this subdivision which can be seen at the top left corner of Figure 9. This is one of the few intense magnetic storms in the 24th solar cycle (Krypiak-Gregorczyk, 2018). This day is a “non-lightning” day as the total lightning counts was less than 10,000. The minimum dst was -103nT which occurred at 23LT as seen in its panel a. PRN 16 which was available at this time recorded a frequency of 0.5mHz, a period of 32 mins and amplitude of 0.1.

3.4.2 No Lightning-Intense Geomagnetic Storm (NL-IS) with no disturbance

20th December 2015 was the day for this pairing which occupies the top right corner of Figure 9. This is one of the few intense magnetic storms in the 24th solar cycle (Krypiak-Gregorczyk, 2018). This day is a “non-lightning” day as the total lightning counts was 0. The minimum dst was -155nT which occurred at 06LT as seen in panel a of this day. PRN 1 which was available at this time recorded a frequency of 0.5mHz, a period of 32 mins and amplitude of 0.01.

3.4.3 No Lightning-Moderate Storm (NL-MS) with disturbance from storm

24th February 2015 was the day for this pairing which can be seen in the middle row of the left column of Figure 9. This day is a “non-lightning” day as the total lightning counts was less than 10,000. The minimum dst was -56nT which occurred at 15LT as seen in panel a of this day. PRN 16 which was available at this time recorded a frequency of 0.9mHz, a period of 18 mins and amplitude of 0.35.

3.4.4 No Lightning-Moderate Storm (NL-MS) with no disturbance

The day for this pairing is 11th September 2015 which is seen at the middle row of the right column. This day is a “non-lightning” day as the total lightning counts was less than 10,000. The minimum dst was -56nT which occurred at 15LT as seen in panel a of this day. PRN 22 which was available at this time recorded a frequency of 0.9mHz, a period of 18 mins and amplitude of 0.02.

3.4.5 No Lightning-Weak Storm (NL-WS) with disturbance from storm

The day for this pairing is 16th November 2015 which occupies the bottom left corner of Figure 9. This day is a "non-lightning" day as the total lightning counts was less than 10,000. The minimum dst was -49nT which occurred at 23LT as seen in panel a of this day. PRN 27 which was available at this time recorded a frequency of 0.5mHz, a period of 32 mins and amplitude of 0.15.

3.4.6 No Lightning-Weak Storm (NL-WS) with disturbance from storm

The day for this pairing is 22nd December 2015 which can be seen at the bottom right corner of Figure 9. The minimum dst was -40nT which occurred at 23LT as seen in its panel a. PRN 22 which was available at this time recorded a frequency of 0.5mHz, a period of 32 mins and amplitude of 0.09.

4 Discussions

This study adds to the body of knowledge of the GNSS-weather event related studies by investigating the ionosphere response to simultaneous and consecutive occurrence of geomagnetic storm and lightning events at various intensities in southern China coastal region. From Table 2 to Table 4 it could be seen that the simultaneous occurrences of these events were almost negligible compared to their consecutive occurrences. On the level of intensity pairings as seen from Table 1, moderate and weak geomagnetic storms were more than intense and super geomagnetic storms. The moderate and weak geomagnetic storms constituted about 90% of the data set. This is because according to Ratovsky et al. (2022), moderate and weak geomagnetic storms which they refer to as standard and recurrent storms tend to happen frequently compared to the intense and super geomagnetic storms. Also, the 24th solar cycle in itself recorded less magnetic storms compared to previous cycles (Patel et al., 2019). This reduces the chance of recording super or intense geomagnetic storms. Thus, following the flow chart of Figure *1*, the intensity pairings (top section of the flow chart) were between the super, intense, moderate and no lighting intensity levels and the moderate and weak intensity levels of geomagnetic storm. That is, all the rows and last three columns of Table 1 were selected for Intensity-Pairing. They were then accessed for the consecutive occurrences (middle section of the flow chart) and finally analyzed according to the bottom section of the flow chart.

From the analysis and results presented in Section 3, despite the different intensity pairings and the subsequent consecutive occurrences, similar trend of observations were made. First, it was realized that both events could cause disturbance or not as seen in Figures 2 to 9. This goes on to show that not all geomagnetic storms or lightning can cause disturbances. A typical example is the St Patrick's Storm on 17th March 2015. Although it was a super geomagnetic storm, it could not cause disturbances. Its effect was like any regular quiet day. The underlying mechanism for such differences begets more studies. One challenge with atmospheric studies is distinguishing which weather event occurred by considering the associated ionospheric disturbance. For example, Ratovsky et al. (2022) attributed the source of same extreme ionospheric events to geomagnetic activity and sudden stratospheric warming (SSW). Also, Yu et al. (2022) reported an increase to about 60TECu during the passage of Typhoon Hato. Other weather events have also been reported to have such similar increment (Suparta & Yusop, 2017). Another observation from this study which provides more evidence to this challenge is that for the times that ROTI exceeded 0.2TECu indicating a disturbance, the ROTI values for both events were mostly between 0.2-0.3TECu. However, the magnitude of the frequency (Fmag) obtained using CWT brings about the much-desired distinction. Fmag was from 0-0.11 when there was no disturbance. It ranged from 0.11 – 0.3 when the disturbance was from geomagnetic storm and further increased to 0.3-0.4 when the disturbance was from lightning only. The main reason for this distinction could be attributed to the frequency at which the highest Fmag is observed. From Figures 2 to 9, it was seen that the highest Fmag was mostly between 0.6-1.1mHz with corresponding period of 18 -25 mins. These are the range of frequency and period at which gravity waves (GW) oscillate (Rahmani et al., 2020). Both geomagnetic storm and lightning are potential sources of GW (Chen et al., 2019). GW is commonly at the bottom ionosphere. Lightning, which is an internal source contributing to MITC is in proximity to the bottom ionosphere thus can generate a bigger magnitude compared to geomagnetic storm which is an external source.

It was expected that the consecutive occurrences could have an influence on the values of Fmag but all the events maintained the same values of disturbance from storm or lightning only. The time difference could allow the disturbed ions and electrons to recombine to restore the ionosphere to its original state (Salem et al., 2015). The ionosphere in restored stated will then respond to another event as usual. Another expectation is that naturally, higher intense levels may have greater impact on the ionosphere. However, that was not the case. Despite Fmag creating a distinction between which event occurred it could not tell apart its level of intensity. The inference is that ionosphere response to various level of intensities may not differ. The similar frequency observed across all intensities for lightning agrees with previous observations that regardless of lighting intensity the dominant frequency is the same (Lay, 2018).

5 Conclusions

The negative effects of space events on GNSS operations have become useful means by which they could be studied to develop early warning and prediction systems to save lives and reduce economic loss. In this study, ionosphere response to simultaneous and consecutive occurrence of geomagnetic storms and lightning events at various intensities were observed using DTEC and ROTI from the Hong Kong network of GNSS receivers. Continuous wavelet transform was used to analyze the DTEC to obtain its frequency and period. When there was no disturbance, the magnitude of the derived frequency was between 0 -0.11.The magnitude was between 0.11-0.3 when the disturbance was from geomagnetic storm only while it increased to 0.3 -0.4 when the disturbance was from lightning only. The respective magnitudes remained the same irrespective of the level of intensity of the event and the order in which they occurred. The differences in magnitude have helped create a distinction to know which event has occurred during ionosphere disturbances. This distinction is a good step for prediction and modelling purposes.

Figure captions

Figure 2: These are the days under the intensity-pairing SL-MS. 4th July 2015, 16th July 2017, 15th August 2015 are for the subdivision “Lightning before geomagnetic storm” showing respectively disturbance from lightning only, disturbance from geomagnetic storm only and no disturbance from both events. 17th March 2016, 1st September 2016, 23rd July 2016 are for the subdivision “Geomagnetic storm before Lightning” showing respectively disturbance from lightning only, disturbance from both events and no disturbance from both events.

Figure 3: These are the days under the intensity-pairing SL-WS. 18th May 2015, 8th September 2016, 6th June 2016 are for the subdivision “Lightning before geomagnetic storm” showing respectively disturbance from lightning only, disturbance from both events and no disturbance from both events. 14th May 2015, 11th June 2015, 19th May 2015, 10th June 2015 are for the subdivision “Geomagnetic storm before Lightning” showing respectively disturbance from geomagnetic storm only, disturbance from both events and no disturbance from both events.

Figure 4: 29th April 2015 and 21st May 2015 are the days under the intensity-pairing SL-NS showing respectively disturbance from lightning and no disturbance. 1st May 2015 and 3rd September are the days under the intensity-pairing IL-NS showing respectively disturbance from lightning and no disturbance. 21st November 2015 and 5th August 2016 are the days under the intensity-pairing ML-NS showing respectively disturbance from lightning and no disturbance.

Figure 5: These are the days under the intensity-pairing IL-MS. 13th April 2016, 8th June 2015 and 17th July 2017 are for the subdivision “Lightning before geomagnetic storm” showing respectively disturbance from geomagnetic storm only, disturbance from both events and no disturbance from both events. 28th September 2017 and 8th May 2016 are for the subdivision “Geomagnetic storm before Lightning” showing respectively disturbance from both events and no disturbance from both events.

Figure 6: These are the days under the intensity-pairing IL-WS. 26th July 2015, 15th June 2015, and 5th September 2016 are for the subdivision “Lightning before geomagnetic storm” showing respectively disturbance from lightning only, disturbance from geomagnetic storm only, and disturbance from both events. 21st August 2014, 14th September 2014, and 19th September 2014 are for the subdivision “Geomagnetic storm before Lightning” showing respectively disturbance from geomagnetic storm only, disturbance from lightning only, and no disturbance from both events.

Figure 7: These are the days under the intensity-pairing ML-MS. 25th June 2015, and 25th October 2015 are for the subdivision “Lightning before geomagnetic storm” showing respectively disturbance from lightning only and no disturbance from both events. 8th September 2015, and 29th September 2016 are for the subdivision “Geomagnetic storm before Lightning” showing respectively disturbance from lightning only and no disturbance from both events.

Figure 8: These are the days under the intensity-pairing ML-WS. 2nd October 2015, 31st March 2017 and 24th April 2017 are for the subdivision “Lightning before geomagnetic storm” showing

respectively disturbance from lightning only, disturbance from both events and no disturbance from both events. 22nd March 2015, 14th July 2015 and 17th June 2015 are for the subdivision "Geomagnetic storm before Lightning" showing respectively disturbance from geomagnetic storm only, disturbance from lightning only, and no disturbance from both events.

Figure 9: 13th October 2016 and 20th December 2015 are the days under the intensity-pairing NL-IS showing respectively disturbance from geomagnetic storm only and no disturbance. 24th February 2015 and 11th September 2015 are the days under the intensity-pairing NL-MS showing respectively disturbance from geomagnetic storm only and no disturbance. 16th November 2015 and 22nd December 2015 are the days under the intensity-pairing NL-WS showing respectively disturbance from lightning and no disturbance.

Acknowledgments

This research was funded by the University Grants Committee of Hong Kong under the scheme Research Impact Fund on the project R5009-21, and the Research Institute of Land and Space, Hong Kong Polytechnic University, and the National Natural Science Foundation of China (Grant number 41804021).The research institutes and government departments where data was obtained for this study are duly acknowledged for their continuous support to scientific studies. The authors also thank the anonymous reviewers for their useful and insightful comments in improving the manuscript.

Open Research and Data Availability Statement

The Dst-index data (IAGA 2002-like format) can be obtained from the Data Analysis Center for Geomagnetism and Space Magnetism, Kyoto University, operating WDC for Geomagnetism, Kyoto (http://wdc.kugi.kyoto-u.ac.jp/dstae/index.html,) (World Data Center for Geomagnetism Kyoto et al., 2015). The Bz component of interplanetary magnetic field was obtained from the GSFC/SPDF OMNIWeb interface at http://omniweb.gsfc.nasa.gov (Papitashvili et al., 2020). The GNSS data can be obtained from Hong Kong SatRef of the Lands Department of the Hong Kong Government (https://www.geodetic.gov.hk/en/rinex/downv.aspx) (Osei-Poku, Tang, Chen, Chen, & Afrifa, 2022). All data center websites were accessed on 14th June 2019.

References

Adhikari, B., Dahal, S., & Chapagain, N. P. (2017). Study of field-aligned current (FAC), interplanetary electric field component (Ey), interplanetary magnetic field component (Bz), and northward (x) and eastward (y) components of geomagnetic field during supersubstorm. *Earth and Space Science, 4*(5), 257-274. https://doi.org/10.1002/2017EA000258

Afraimovich, E. L., Astafyeva, E. I., Demyanov, V. V., Edemskiy, I. K., Gavrilyuk, N. S., Ishin, A. B., Kosogorov, E. A., Leonovich, L. A., Lesyuta, O. S., Palamartchouk, K. S., Perevalova, N. P., Polyakova, A. S., Smolkov, G. Y., Voeykov, S. V., Yasyukevich, Y. V., & Zhivetiev, I. V. (2013). A review of GPS/GLONASS studies of the ionospheric response to natural and anthropogenic processes and phenomena. *Journal of Space Weather and Space Climate, 3*. https://doi.org/10.1051/swsc/2013049

Amin, M. M. (2015). *Influence of lightning on electron density variation in the ionosphere using WWLLN lightning data and GPS data* [Masters Thesis, University of Cape Town]. OpenUCT. http://hdl.handle.net/11427/13565

Borries, C., Jakowski, N., & Wilken, V. (2009). Storm induced large scale TIDs observed in GPS derived TEC. *Annales Geophysicae, 27*(4), 1605-1612. https://doi.org/10.5194/angeo-27-1605-2009

Chane-Ming, F., Molinaro, F., Leveau, J., Keckhut, P., & Hauchecorne, A. (2000). Analysis of gravity waves in the tropical middle atmosphere over La Reunion Island (21°S, 55°E) with lidar using wavelet techniques. *Ann. Geophys., 18*(4), 485-498. https://doi.org/10.1007/s00585-000-0485-0

Chen, G., Zhou, C., Liu, Y., Zhao, J., Tang, Q., Wang, X., & Zhao, Z. (2019). A statistical analysis of medium-scale traveling ionospheric disturbances during 2014–2017 using the Hong Kong CORS network. *Earth, Planets and Space, 71*(1). https://doi.org/10.1186/s40623-019-1031-9

Chen, J., Zhang, X., Ren, X., Zhang, J., Freeshah, M., & Zhao, Z. (2020). Ionospheric disturbances detected during a typhoon based on GNSS phase observations: A case study for typhoon Mangkhut over Hong Kong. *Advances in Space Research, 66*(7), 1743-1753. https://doi.org/10.1016/j.asr.2020.06.006

Cherniak, I., & Zakharenkova, I. (2018). Large-Scale Traveling Ionospheric Disturbances Origin and Propagation: Case Study of the December 2015 Geomagnetic Storm. *Space Weather, 16*(9), 1377-1395. https://doi.org/10.1029/2018sw001869

Ding, F., Wan, W., Ning, B., & Wang, M. (2007). Large-scale traveling ionospheric disturbances observed by GPS total electron content during the magnetic storm of 29-30 October 2003. *Journal of Geophysical Research: Space Physics, 112*(6), 1-15. https://doi.org/10.1029/2006JA012013

Kong, J., Yao, Y., Zhou, C., Liu, Y., Zhai, C., Wang, Z., & Liu, L. (2018). Tridimensional reconstruction of the Co-Seismic Ionospheric Disturbance around the time of 2015 Nepal earthquake. *Journal of Geodesy, 92*(11), 1255-1266. https://doi.org/10.1007/s00190-018-1117-3

Krypiak-Gregorczyk, A. (2018). Ionosphere response to three extreme events occurring near spring equinox in 2012, 2013 and 2015, observed by regional GNSS-TEC model. *Journal of Geodesy*. https://doi.org/10.1007/s00190-018-1216-1

Lay, E. H. (2018). Ionospheric Irregularities and Acoustic/Gravity Wave Activity Above Low-Latitude Thunderstorms. *Geophysical Research Letters, 45*(1), 90-97. https://doi.org/10.1002/2017GL076058

Liu, T., Yu, Z., Ding, Z., Nie, W., & Xu, G. (2021). Observation of Ionospheric Gravity Waves Introduced by Thunderstorms in Low Latitudes China by GNSS. *Remote Sensing, 13*(20), 4131. https://doi.org/10.3390/rs13204131

Loewe, C. A. (1997). Classification and mean behavior of magnetic storms. *Journal of Geophysical Research A: Space Physics, 102*(A7), 14209-14213. https://doi.org/10.1029/96JA04020

McGranaghan, R. M., Mannucci, A. J., & Forsyth, C. (2017). A Comprehensive Analysis of Multiscale Field-Aligned Currents: Characteristics, Controlling Parameters, and Relationships. *Journal of Geophysical Research: Space Physics, 122*(12), 11931-11960. https://doi.org/10.1002/2017JA024742

Ogunsua, B. O., Srivastava, A., Bian, J., Qie, X., Wang, D., Jiang, R., & Yang, J. (2020, May 21). Significant Day-time Ionospheric Perturbation by Thunderstorms along the West African and Congo Sector of Equatorial Region. *Sci Rep, 10*(1), 8466. https://doi.org/10.1038/s41598-020-65315-3

Osei-Poku, L., Tang, L., Chen, W., Chen, M., & Acheampong, A. A. (2022). Comparative Study of Predominantly Daytime and Nighttime Lightning Occurrences and Their Impact on Ionospheric Disturbances. *Remote Sensing, 14*(13). https://doi.org/10.3390/rs14133209

Osei-Poku, L., Tang, L., Chen, W., Chen, M., & Afrifa, A. A. (2022). *Rinex files from the Hong Kong GNSS network [dataset]*. https://doi.org/10.5281/zenodo.7431366

Osei-Poku, L., Tang, L., Chen, W., & Mingli, C. (2021). Evaluating Total Electron Content (TEC) Detrending Techniques in Determining Ionospheric Disturbances during Lightning Events in A Low Latitude Region. *Remote Sensing, 13*(23). https://doi.org/10.3390/rs13234753

Papitashvili, Natalia, E., & King, J. H. (2020). *"OMNI Hourly Data" [Data Set]* NASA Space Physics Data Facility. https://doi.org/10.48322/1shr-ht18

Patel, K., Singh, A., Singh, S. B., & Singh, A. K. (2019). Causes responsible for intense and severe storms during the declining phase of Solar Cycle 24. *Journal of Astrophysics and Astronomy, 40*(1), 1-9. https://doi.org/10.1007/s12036-018-9569-7

Pi, X., Mannucci, A. J., Lindqwister, U. J., & Ho, C. M. (1997). Monitoring of global ionospheric irregularities using the worldwide GPS network. *Geophysical Research Letters, 24*(18), 2283-2286. https://doi.org/10.1029/97GL02273

Qin, Z., Chen, M., Lyu, F., Cummer, S. A., Gao, Y., Liu, F., Zhu, B., Du, Y. p., Usmani, A., & Qiu, Z. (2020). Prima Facie Evidence of the Fast Impact of a Lightning Stroke on the Lower Ionosphere. *Geophysical Research Letters, 47*(21), e2020GL090274. https://doi.org/10.1029/2020gl090274

Rahmani, Y., Alizadeh, M. M., Schuh, H., Wickert, J., & Tsai, L.-C. (2020). Probing vertical coupling effects of thunderstorms on lower ionosphere using GNSS data. *Advances in Space Research, 66*(8), 1967-1976. https://doi.org/10.1016/j.asr.2020.07.018

Ratovsky, K. G., Klimenko, M. V., Dmitriev, A. V., & Medvedeva, I. V. (2022). Relation of Extreme Ionospheric Events with Geomagnetic and Meteorological Activity. *Atmosphere, 13*(1).

Salem, M. A., Liu, N., & Rassoul, H. K. (2015). Effects of small thundercloud electrostatic fields on the ionospheric density profile. *Geophysical Research Letters, 42*(6), 1619-1625. https://doi.org/10.1002/2015GL063268

Suparta, W., & Yusop, N. (2017, 2017/05). Response of lightning energy and total electron content with sprites over Antarctic Peninsula. Journal of Physics: Conference Series, Tang, L., Chen, W., Chen, M., & Osei-Poku, L. (2019). Statistical observation of thunderstorm-induced ionospheric Gravity waves above low-latitude areas in the northern hemisphere. *Remote Sensing, 11*(23), 2732. https://doi.org/10.3390/rs11232732

World Data Center for Geomagnetism Kyoto, Nose, M., Iyemori, T., Sugiura, M., & Kamei, T. (2015). *Geomagnetic Dst index [Dataset]*. https://doi.org/10.17593/14515-74000

Wu, Q., Chou, M.-Y., Schreiner, W., Braun, J., Pedatella, N., & Cherniak, I. (2021). COSMIC observation of stratospheric gravity wave and ionospheric scintillation correlation. *Journal of Atmospheric and Solar-Terrestrial Physics, 217*, 105598. https://doi.org/10.1016/j.jastp.2021.105598

Yang, Z., & Liu, Z. (2016). Correlation between ROTI and Ionospheric Scintillation Indices using Hong Kong low-latitude GPS data. *GPS Solutions, 20*(4), 815-824. https://doi.org/10.1007/s10291-015-0492-y

Yu, S., & Liu, Z. (2021). The ionospheric condition and GPS positioning performance during the 2013 tropical cyclone Usagi event in the Hong Kong region. *Earth, Planets and Space, 73*(1), 1-16. https://doi.org/10.1186/s40623-021-01388-2

Yu, S., Liu, Z., & Lee, T. C. (2022, 2022/01/01). Ionospheric Disturbances Observed From a Single GPS Station in Hong Kong During the Passage of Super Typhoon Hato in 2017 [https://doi.org/10.1029/2021SW002850]. *Space Weather, 20*(1), e2021SW002850. https://doi.org/https://doi.org/10.1029/2021SW002850

Flow Chart of the Data Groupings.

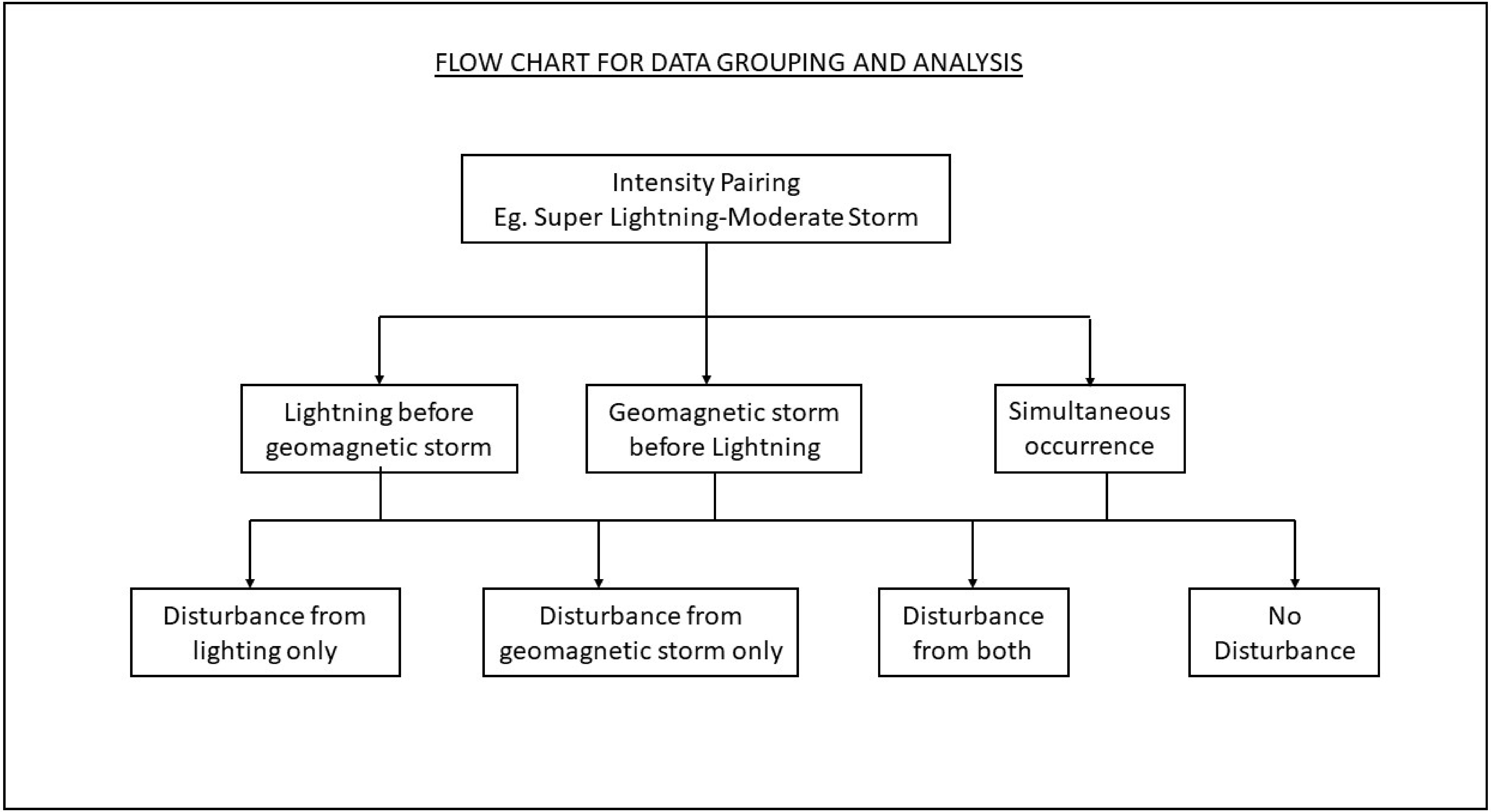
FLOW CHART FOR DATA GROUPING AND ANALYSIS
Intensity Pairing
Eg. Super Lightning-Moderate Storm
Lightning before geomagnetic storm
Geomagnetic storm before Lightning
Simultaneous occurrence
Disturbance from lighting only
Disturbance from geomagnetic storm only
Disturbance from both
No Disturbance

Figure 2: These are the days under the intensity-pairing SL-MS. 4th July 2015, 16th July 2017, 15th August 2015 are for the subdivision "Lightning before geomagnetic storm" showing respectively distur.

LIGHTNING BEFORE GEOMAGNETIC STORM

GEOMAGNETIC STORM BEFORE LIGHTNING

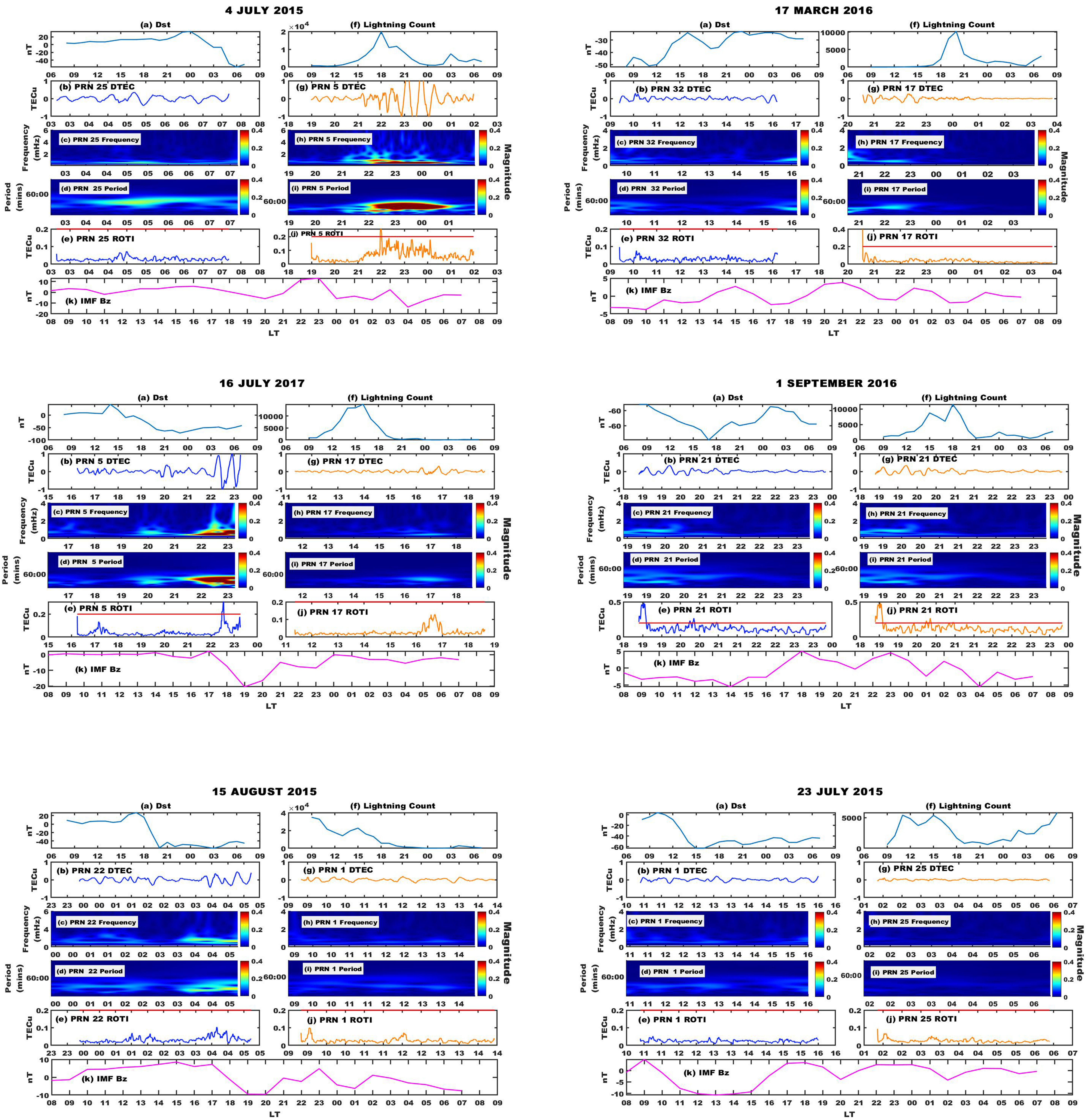

Figure 3: These are the days under the intensity-pairing SL-WS. 18th May 2015, 8th September 2016, 6th June 2016 are for the subdivision "Lightning before geomagnetic storm" showing respectively distu.

LIGHTNING BEFORE GEOMAGNETIC STORM

GEOMAGNETIC STORM BEFORE LIGHTNING

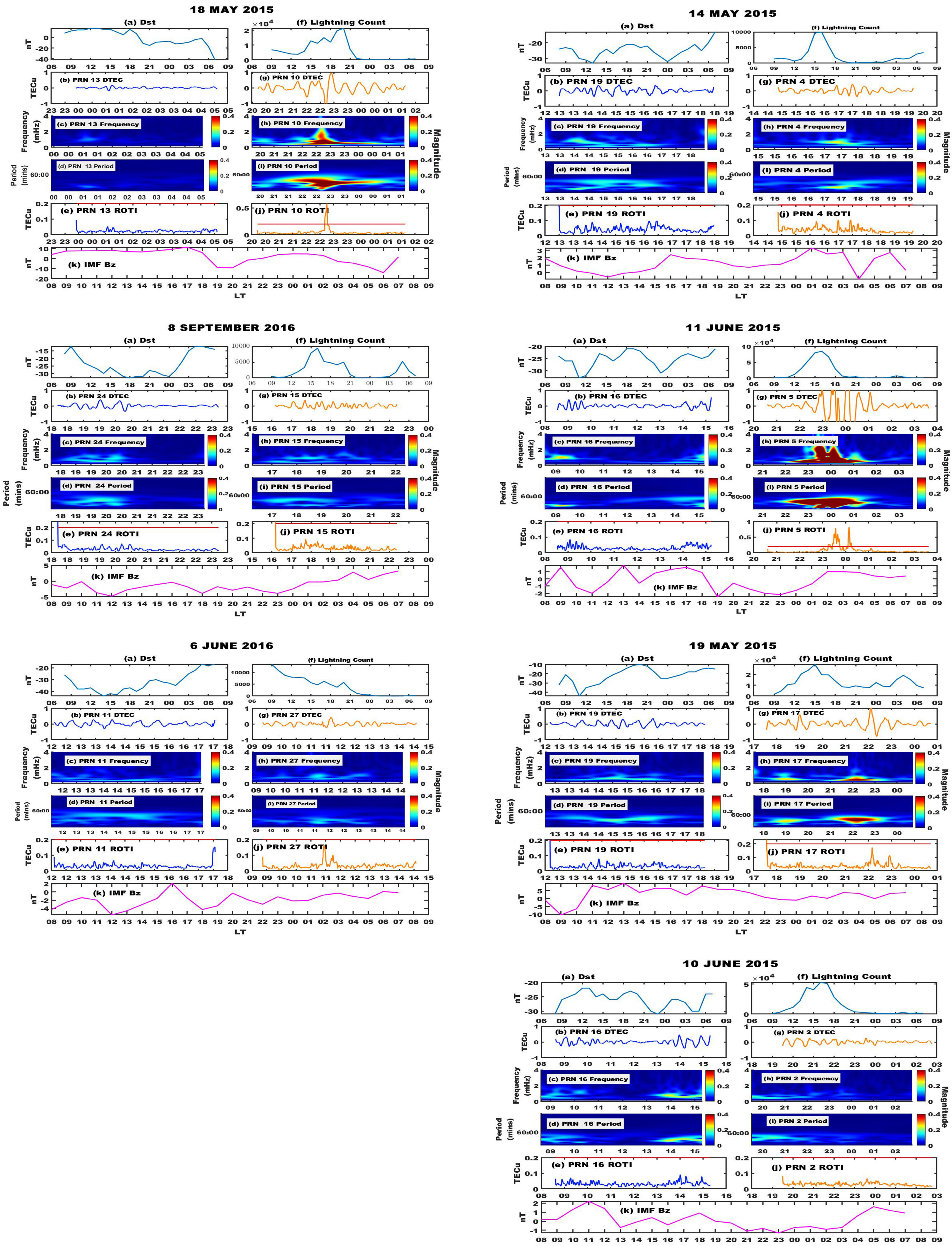

Figure 4: 29th April 2015 and 21st May 2015 are the days under the intensity-pairing SL-NS showing respectively disturbance from lightning and no disturbance. 1st May 2015 and 3rd September are the da.

SUPER LIGHTNING - NO GEOMAGNETIC STORM (SL-NS)

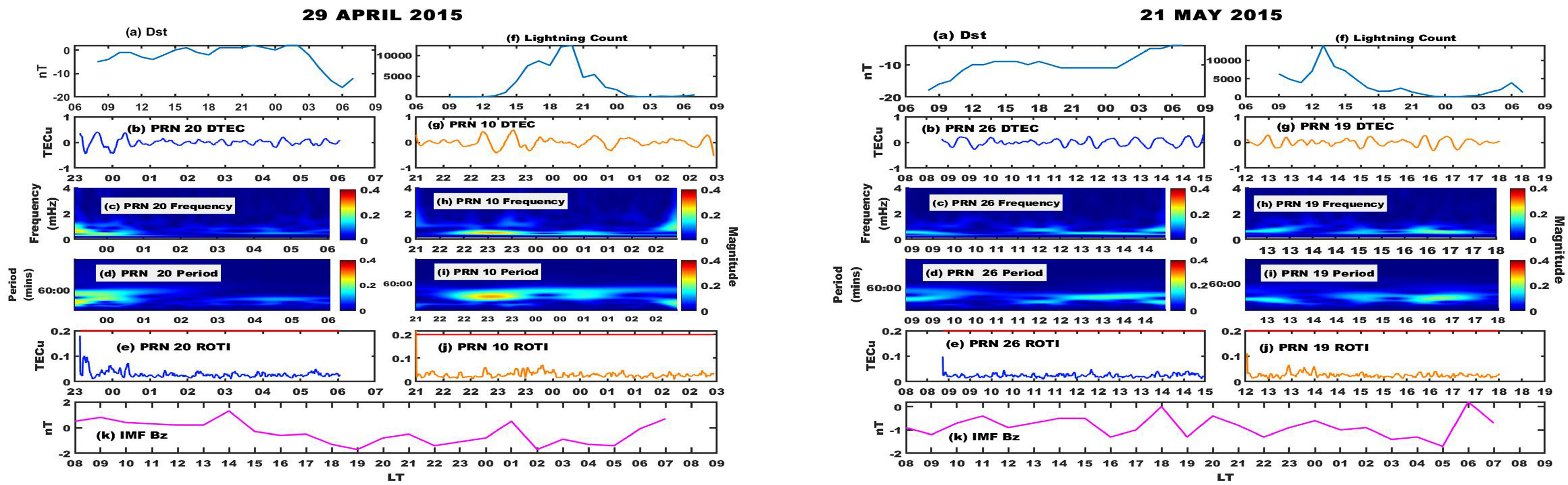

INTENSE LIGHTNING - NO GEOMAGNETIC STORM (IL-NS)

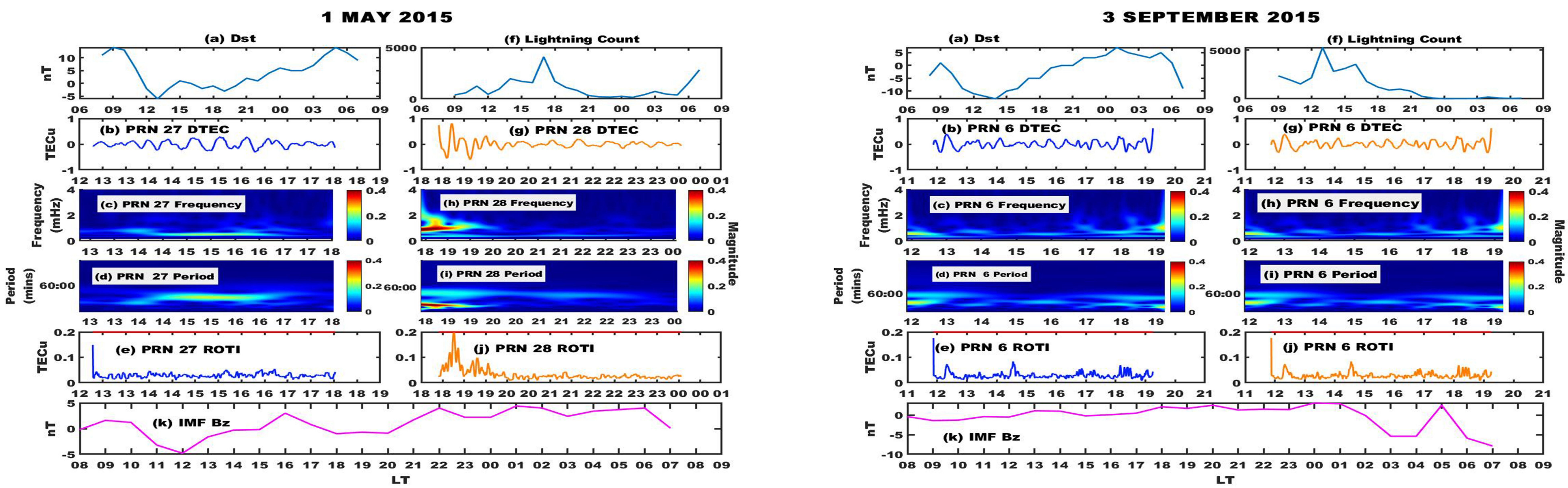

MODERATE LIGHTNING - NO GEOMAGNETIC STORM (ML-NS)

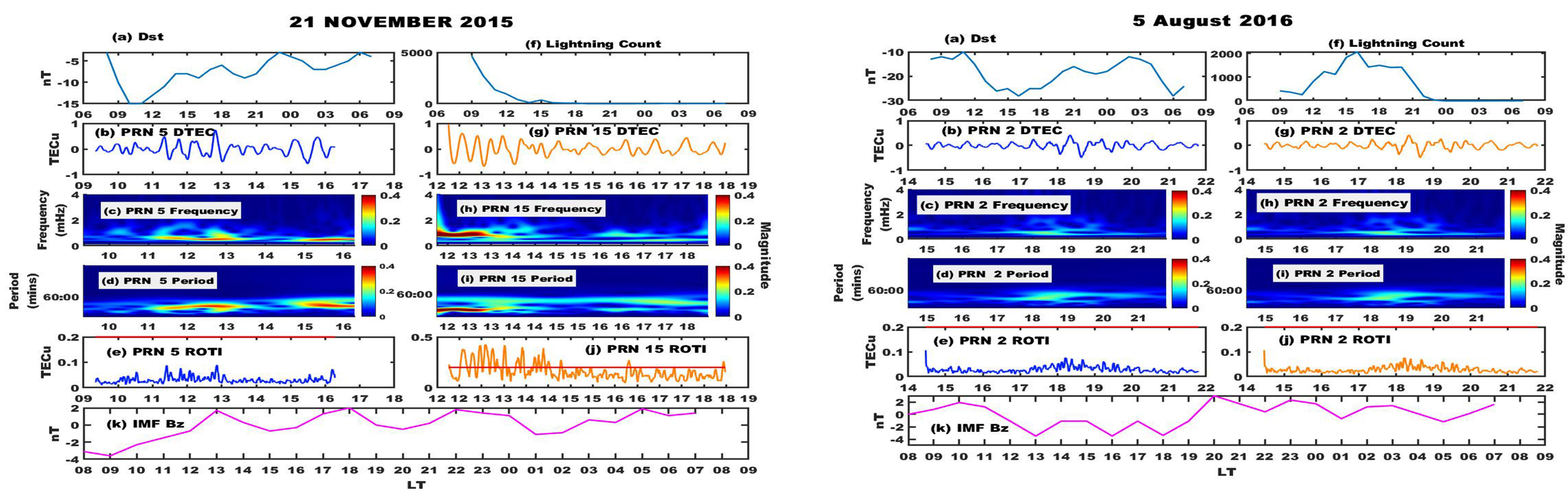

Figure 5: These are the days under the intensity-pairing IL-MS. 13th April 2016, 8th June 2015 and 17th July 2017 are for the subdivision "Lightning before geomagnetic storm" showing respectively dist.

LIGHTNING BEFORE GEOMAGNETIC STORM

GEOMAGNETIC STORM BEFORE LIGHTNING

13 APRIL 2016

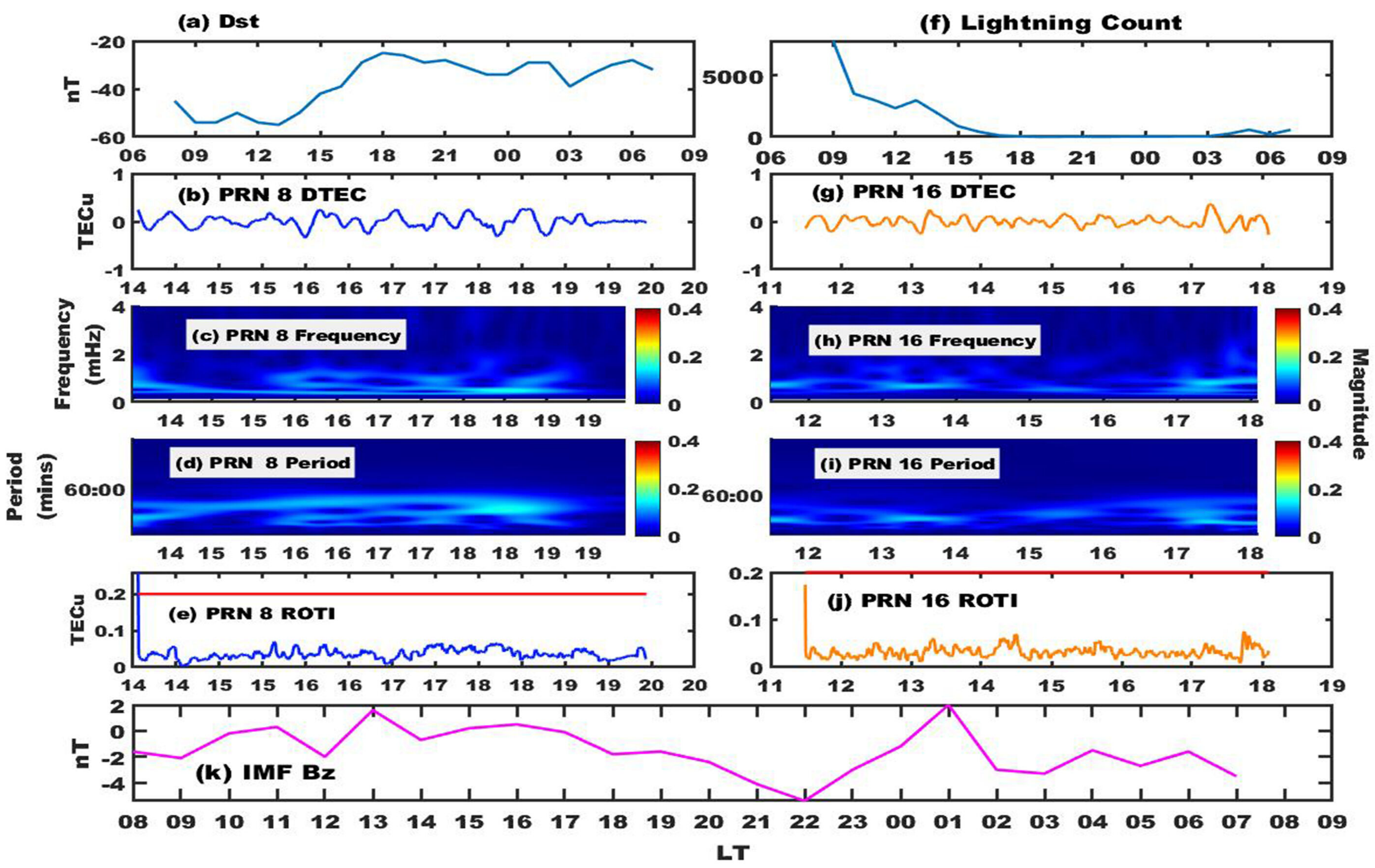

28 SEPTEMBER 2017

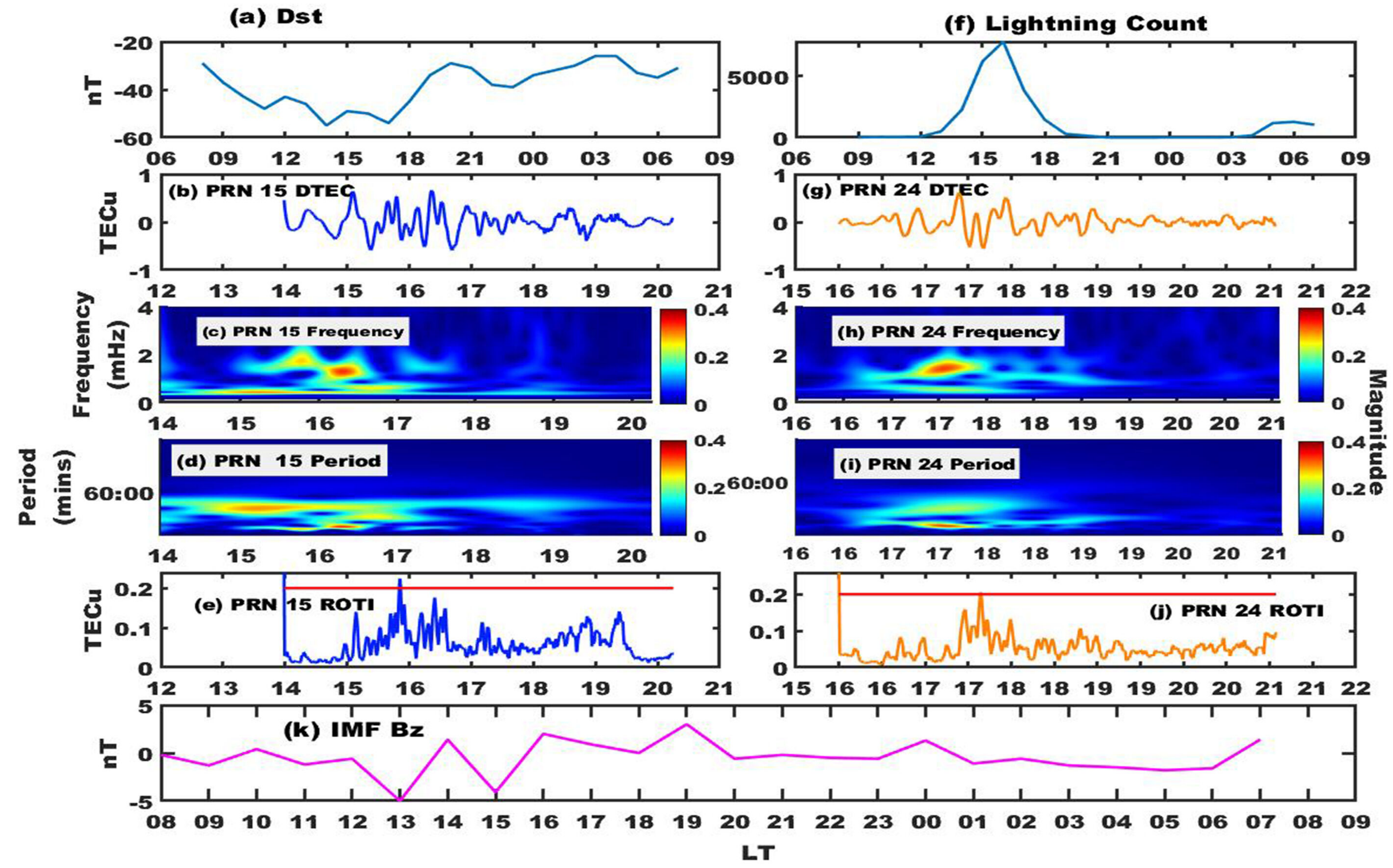

8 JUNE 2015

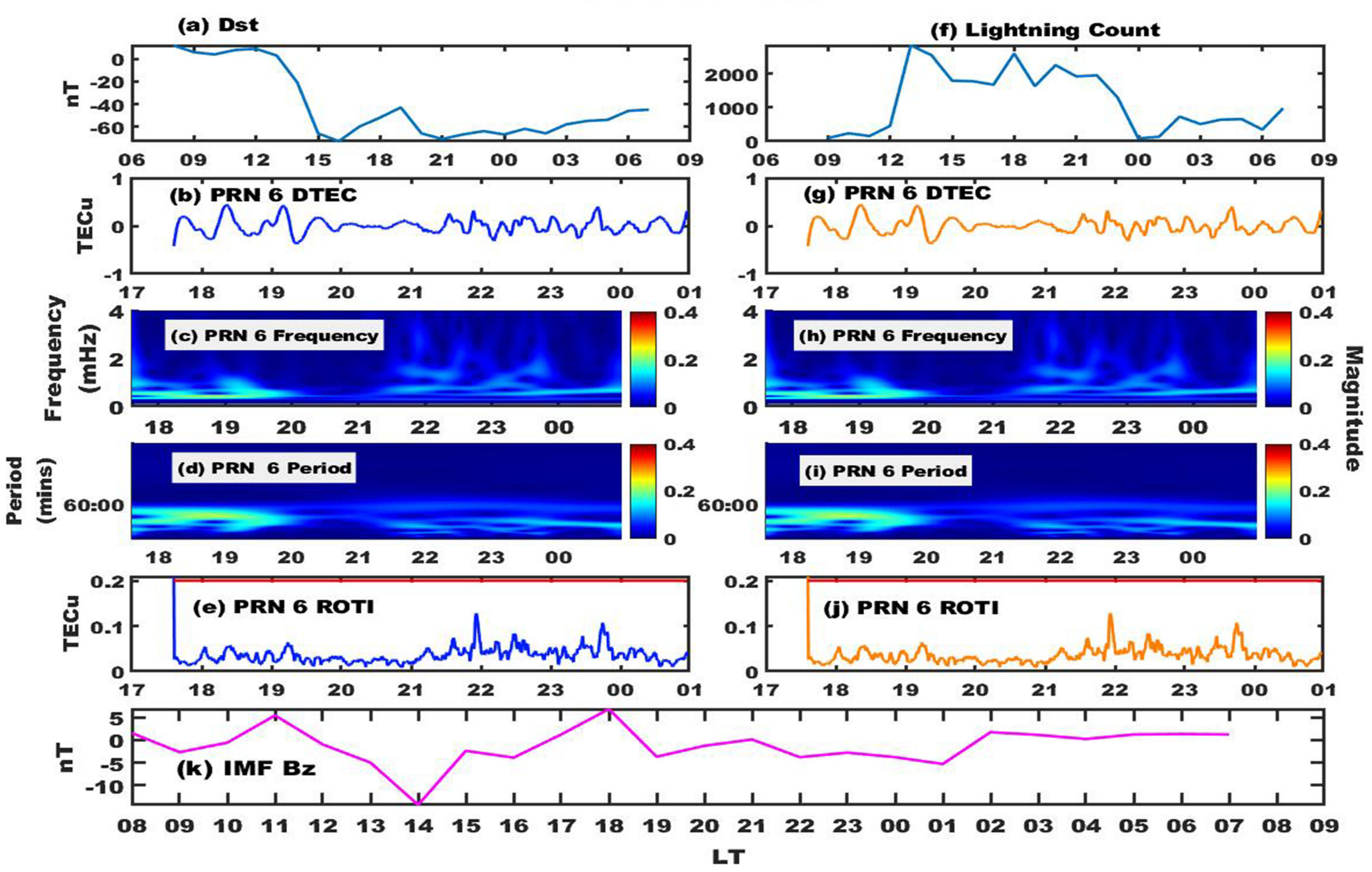

8 MAY 2016

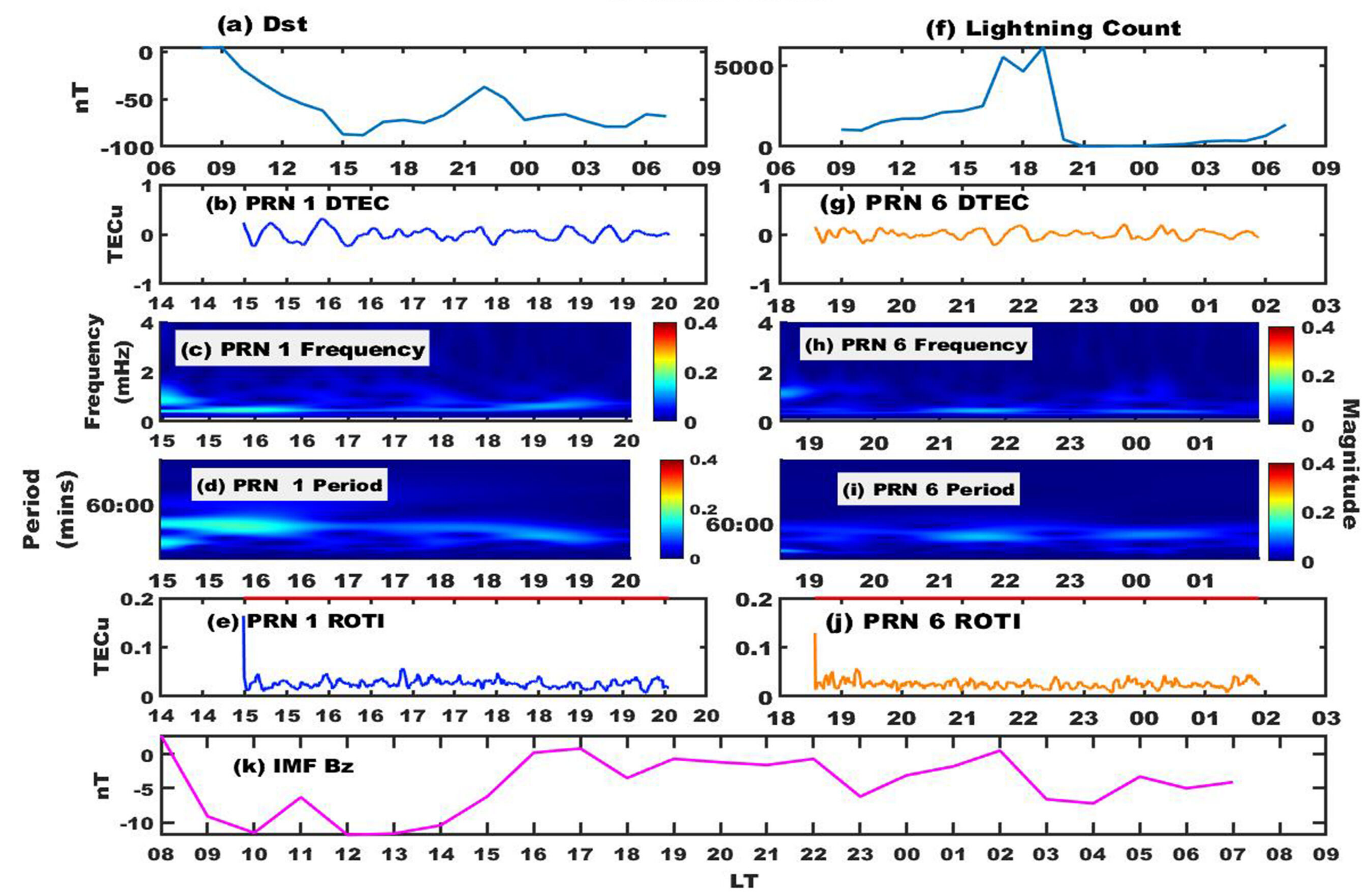

17 JULY 2017

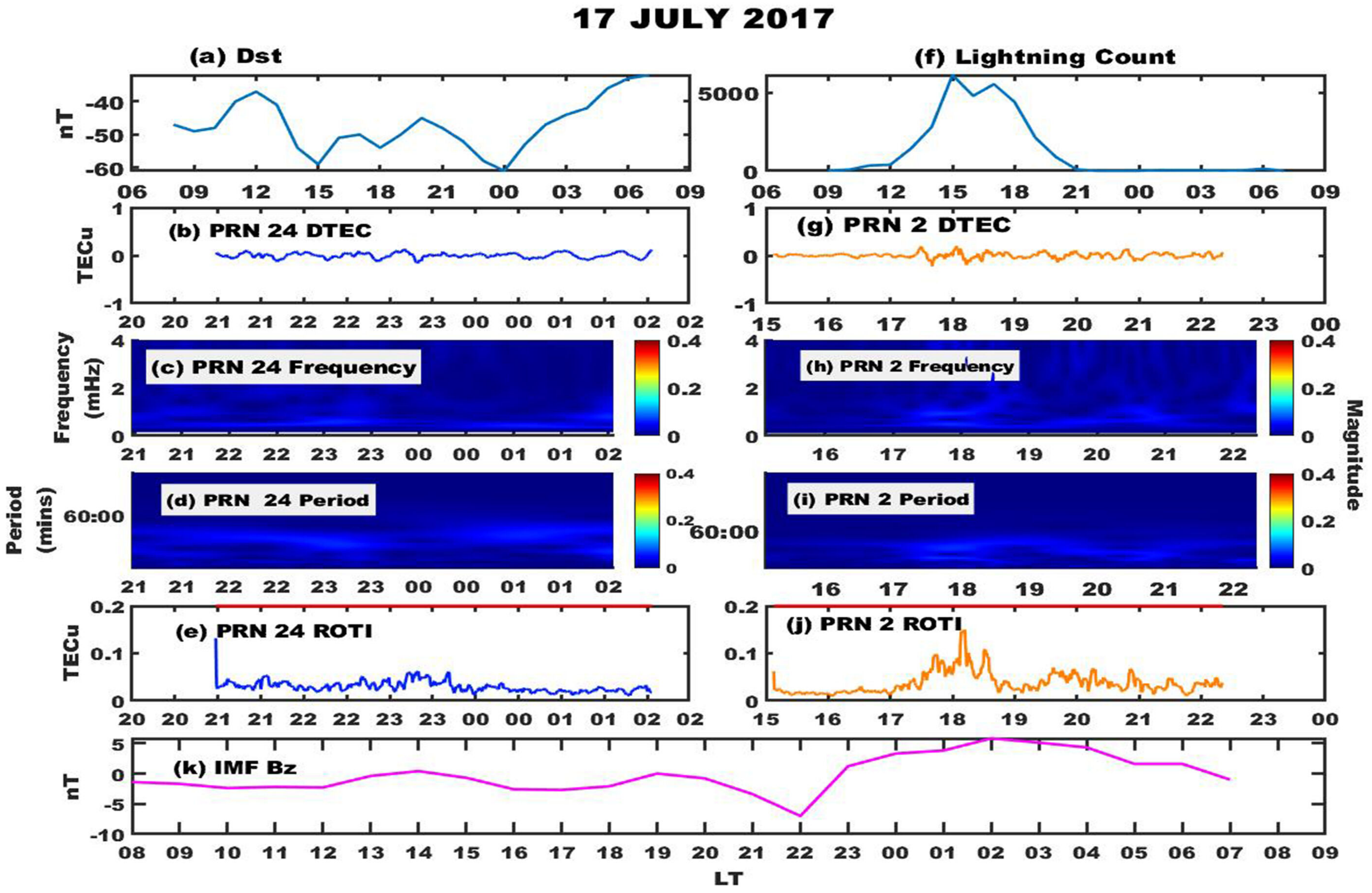

Figure 6: These are the days under the intensity-pairing IL-WS. 26th July 2015, 15th June 2015, and 5th September 2016 are for the subdivision "Lightning before geomagnetic storm" showing respectively.

LIGHTNING BEFORE GEOMAGNETIC STORM

GEOMAGNETIC STORM BEFORE LIGHTNING

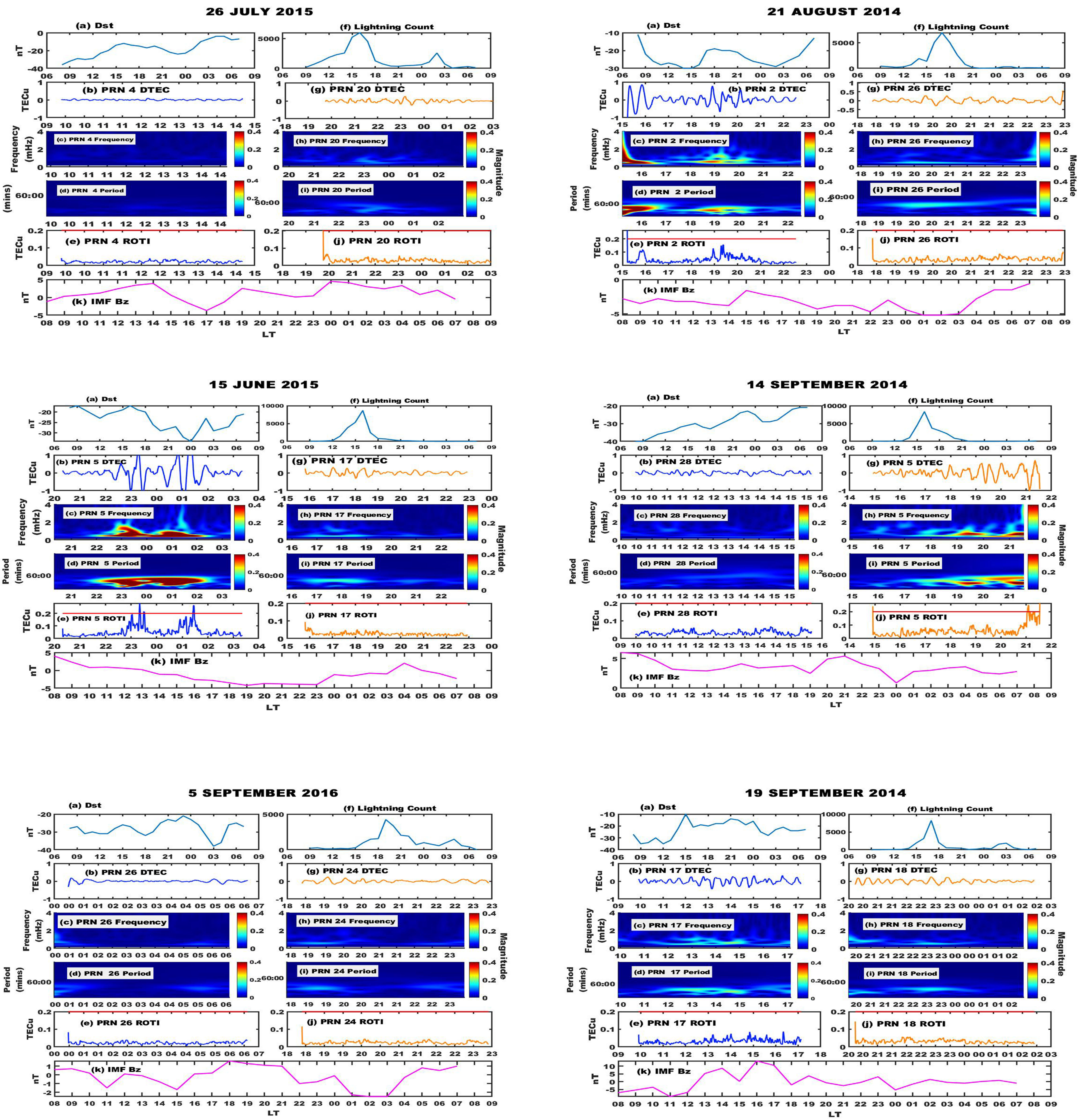

Figure 7: These are the days under the intensity-pairing ML-MS. 25th June 2015, and 25th October 2015 are for the subdivision "Lightning before geomagnetic storm" showing respectively disturbance from.

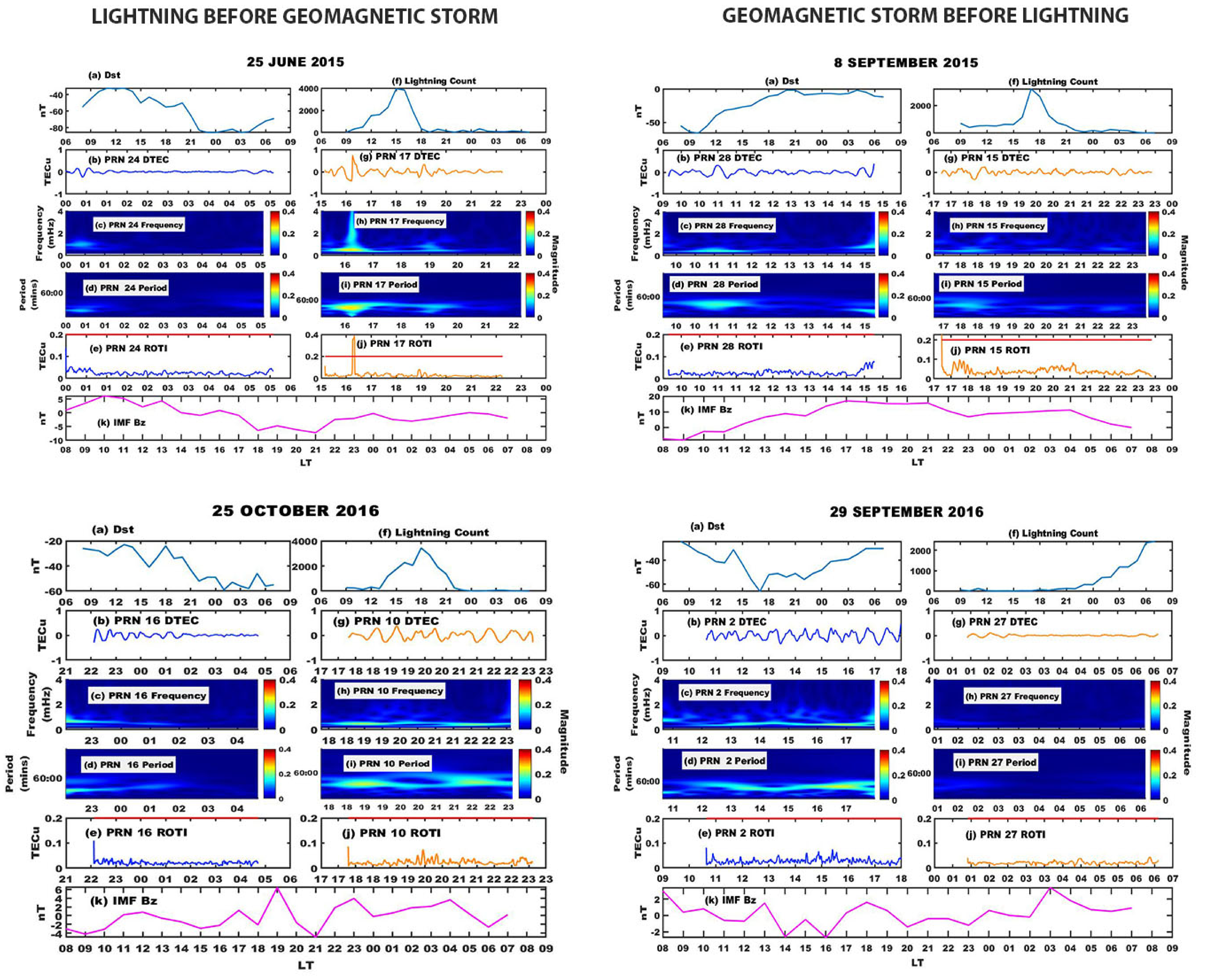

LIGHTNING BEFORE GEOMAGNETIC STORM
GEOMAGNETIC STORM BEFORE LIGHTNING
25 JUNE 2015
(a) Dst
(f) Lightning Count
(b) PRN 24 DTEC
(g) PRN 17 DTEC
(c) PRN 24 Frequency
(h) PRN 17 Frequency
(d) PRN 24 Period
(i) PRN 17 Period
(e) PRN 24 ROTI
(j) PRN 17 ROTI
(k) IMF Bz
8 SEPTEMBER 2015
(a) Dst
(f) Lightning Count
(b) PRN 28 DTEC
(g) PRN 15 DTEC
(c) PRN 28 Frequency
(h) PRN 15 Frequency
(d) PRN 28 Period
(i) PRN 15 Period
(e) PRN 28 ROTI
(j) PRN 15 ROTI
(k) IMF Bz
25 OCTOBER 2016
(a) Dst
(f) Lightning Count
(b) PRN 16 DTEC
(g) PRN 10 DTEC
(c) PRN 16 Frequency
(h) PRN 10 Frequency
(d) PRN 16 Period
(i) PRN 10 Period
(e) PRN 16 ROTI
(j) PRN 10 ROTI
(k) IMF Bz
29 SEPTEMBER 2016
(a) Dst
(f) Lightning Count
(b) PRN 2 DTEC
(g) PRN 27 DTEC
(c) PRN 2 Frequency
(h) PRN 27 Frequency
(d) PRN 2 Period
(i) PRN 27 Period
(e) PRN 2 ROTI
(j) PRN 27 ROTI
(k) IMF Bz
nT
TECu
Frequency (mHz)
Period (mins)
Magnitude
LT

Figure 8: These are the days under the intensity-pairing ML-WS. 2nd October 2015, 31st March 2017 and 24th April 2017 are for the subdivision "Lightning before geomagnetic storm" showing respectively.

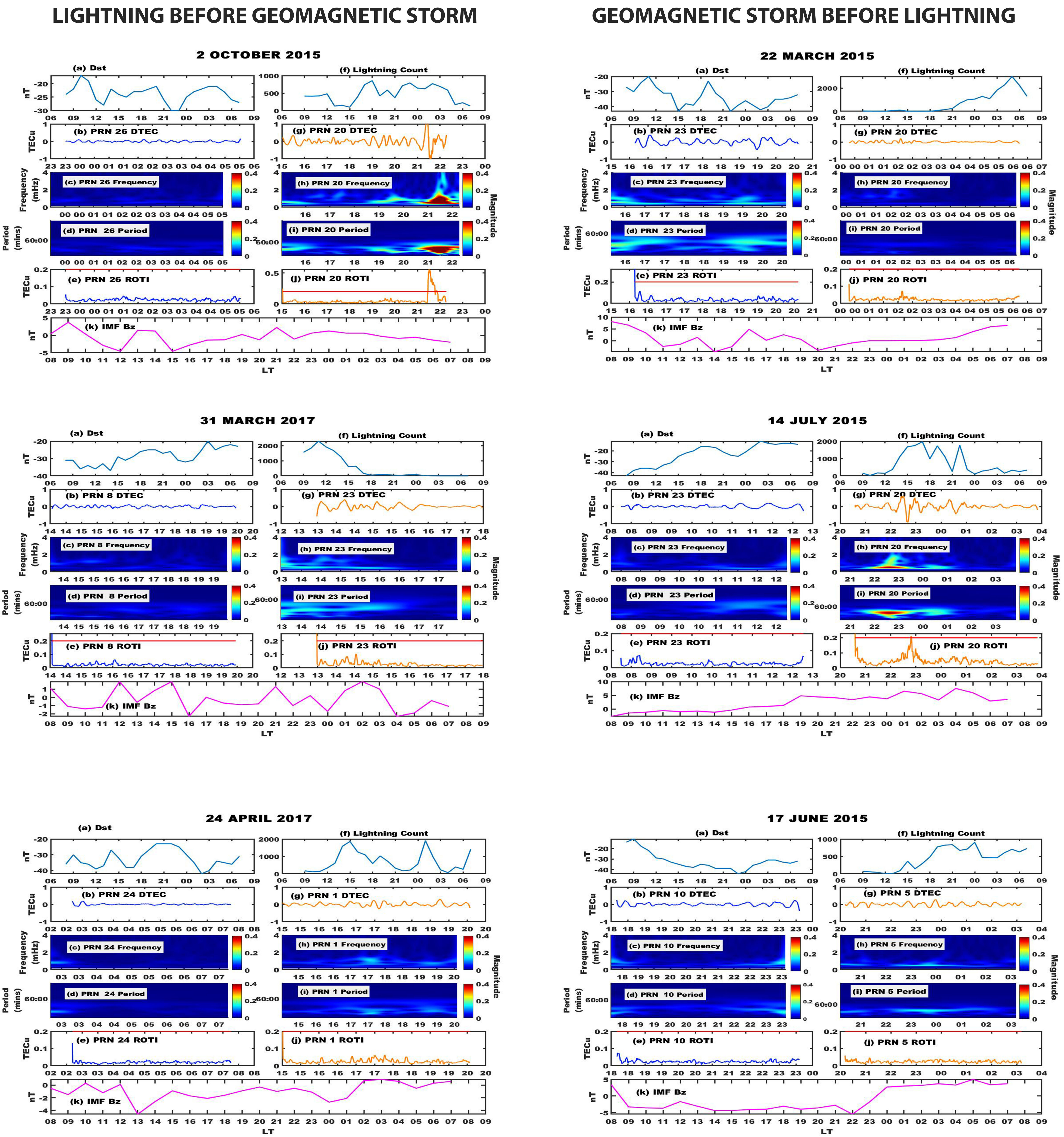
LIGHTNING BEFORE GEOMAGNETIC STORM
GEOMAGNETIC STORM BEFORE LIGHTNING
2 OCTOBER 2015
(a) Dst
(f) Lightning Count
(b) PRN 26 DTEC
(g) PRN 20 DTEC
(c) PRN 26 Frequency
(h) PRN 20 Frequency
(d) PRN 26 Period
(i) PRN 20 Period
(e) PRN 26 ROTI
(j) PRN 20 ROTI
(k) IMF Bz
22 MARCH 2015
(a) Dst
(f) Lightning Count
(b) PRN 23 DTEC
(g) PRN 20 DTEC
(c) PRN 23 Frequency
(h) PRN 20 Frequency
(d) PRN 23 Period
(i) PRN 20 Period
(e) PRN 23 ROTI
(j) PRN 20 ROTI
(k) IMF Bz
31 MARCH 2017
(a) Dst
(f) Lightning Count
(b) PRN 8 DTEC
(g) PRN 23 DTEC
(c) PRN 8 Frequency
(h) PRN 23 Frequency
(d) PRN 8 Period
(i) PRN 23 Period
(e) PRN 8 ROTI
(j) PRN 23 ROTI
(k) IMF Bz
14 JULY 2015
(a) Dst
(f) Lightning Count
(b) PRN 23 DTEC
(g) PRN 20 DTEC
(c) PRN 23 Frequency
(h) PRN 20 Frequency
(d) PRN 23 Period
(i) PRN 20 Period
(e) PRN 23 ROTI
(j) PRN 20 ROTI
(k) IMF Bz
24 APRIL 2017
(a) Dst
(f) Lightning Count
(b) PRN 24 DTEC
(g) PRN 1 DTEC
(c) PRN 24 Frequency
(h) PRN 1 Frequency
(d) PRN 24 Period
(i) PRN 1 Period
(e) PRN 24 ROTI
(j) PRN 1 ROTI
(k) IMF Bz
17 JUNE 2015
(a) Dst
(f) Lightning Count
(b) PRN 10 DTEC
(g) PRN 5 DTEC
(c) PRN 10 Frequency
(h) PRN 5 Frequency
(d) PRN 10 Period
(i) PRN 5 Period
(e) PRN 10 ROTI
(j) PRN 5 ROTI
(k) IMF Bz
nT
TECu
Frequency (mHz)
Period (mins)
Magnitude
LT

Figure 9: 13th October 2016 and 20th December 2015 are the days under the intensity-pairing NL-IS showing respectively disturbance from geomagnetic storm only and no disturbance. 24th February 2015 an.

NO LIGHTNING - INTENSE GEOMAGNETIC STORM (NL-IS)

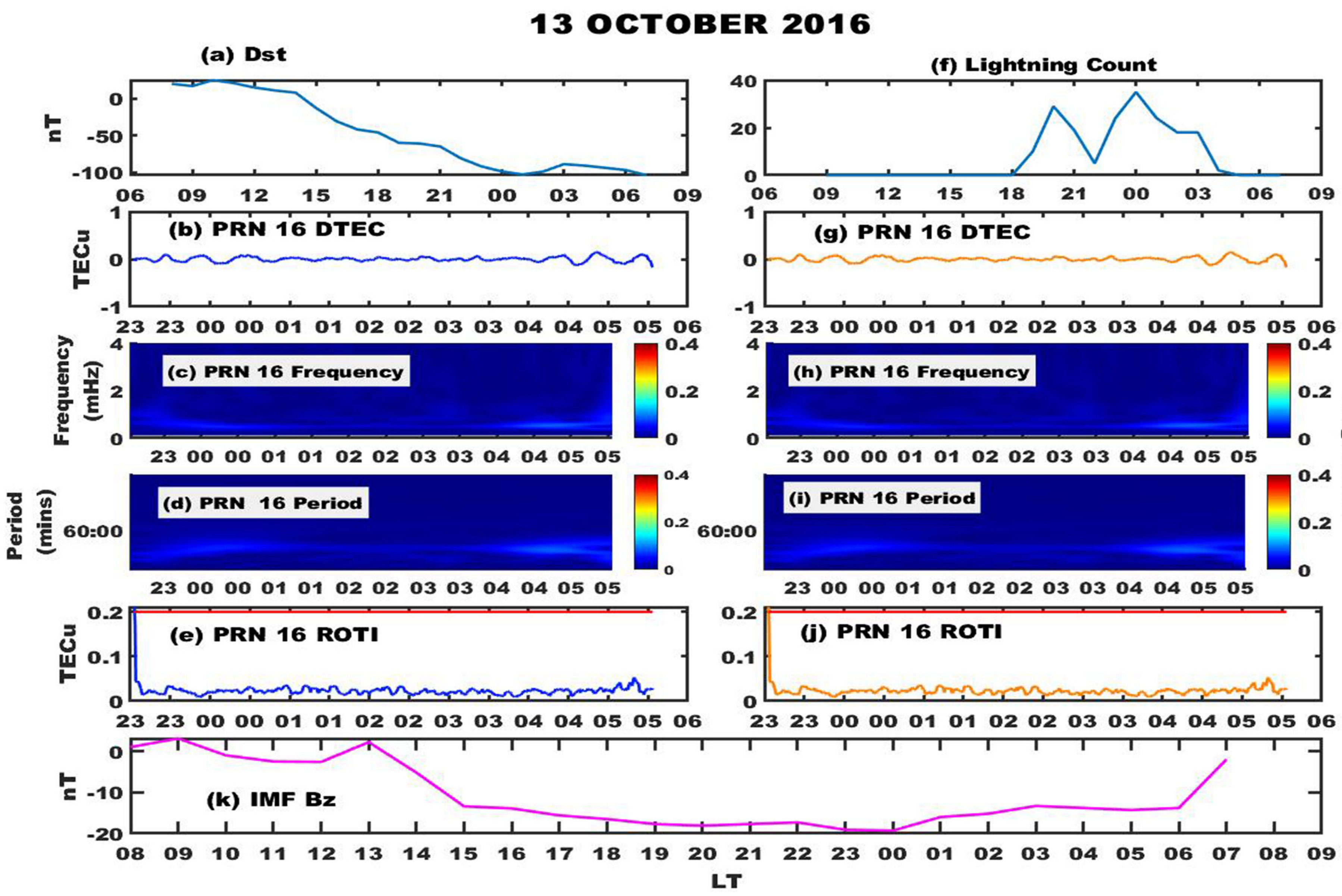

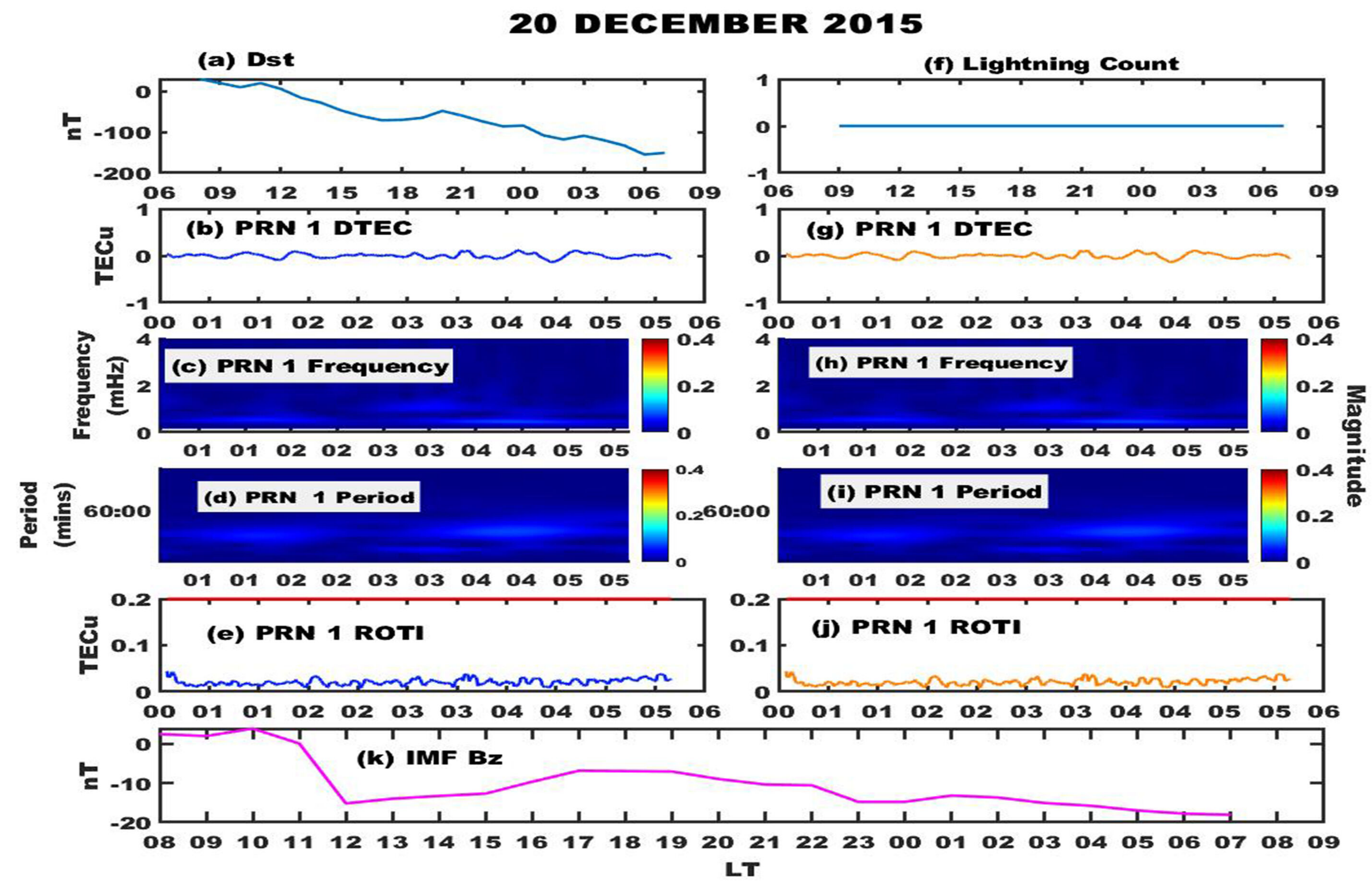

NO LIGHTNING - MODERATE GEOMAGNETIC STORM (NL-MS)

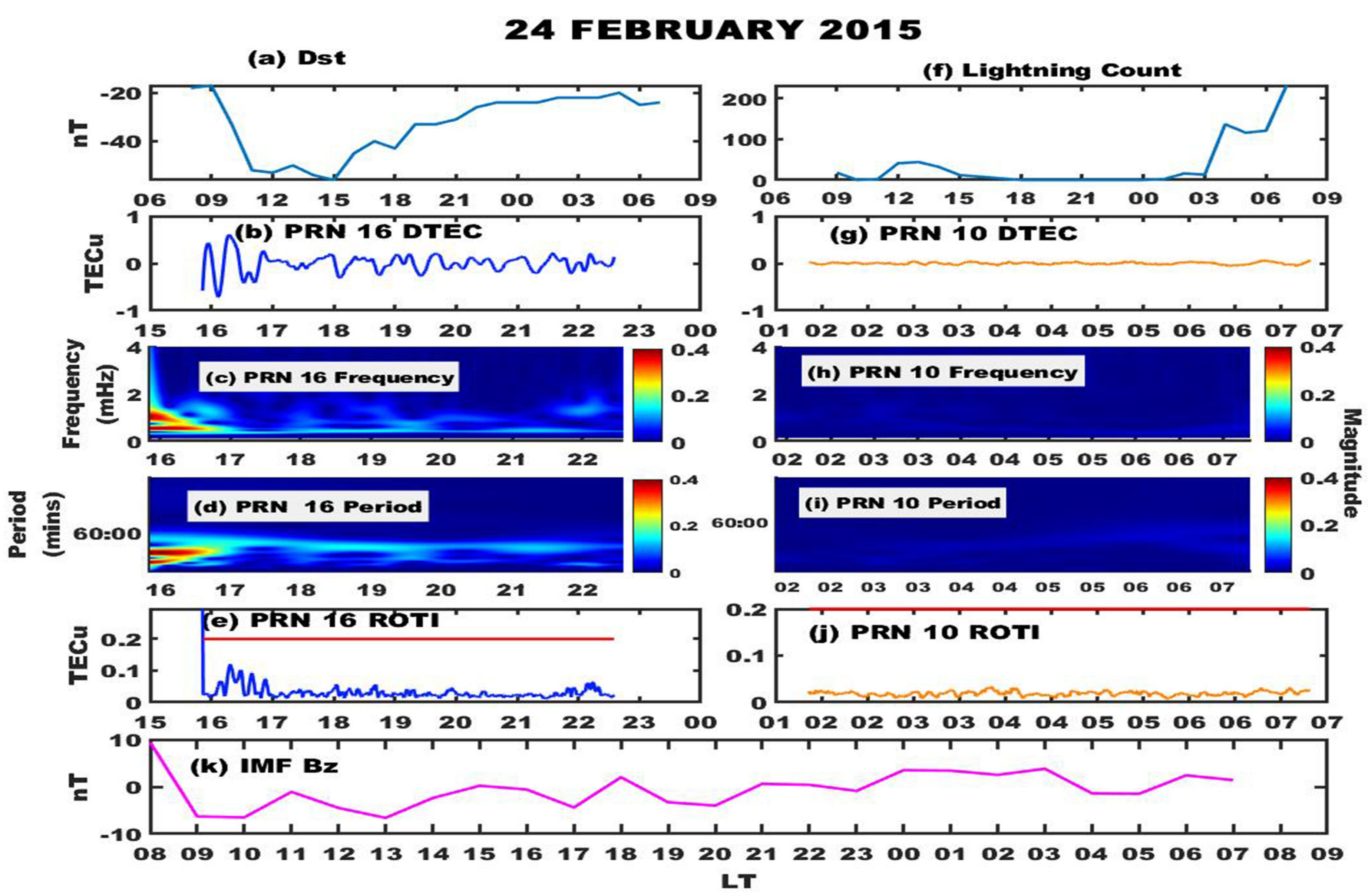

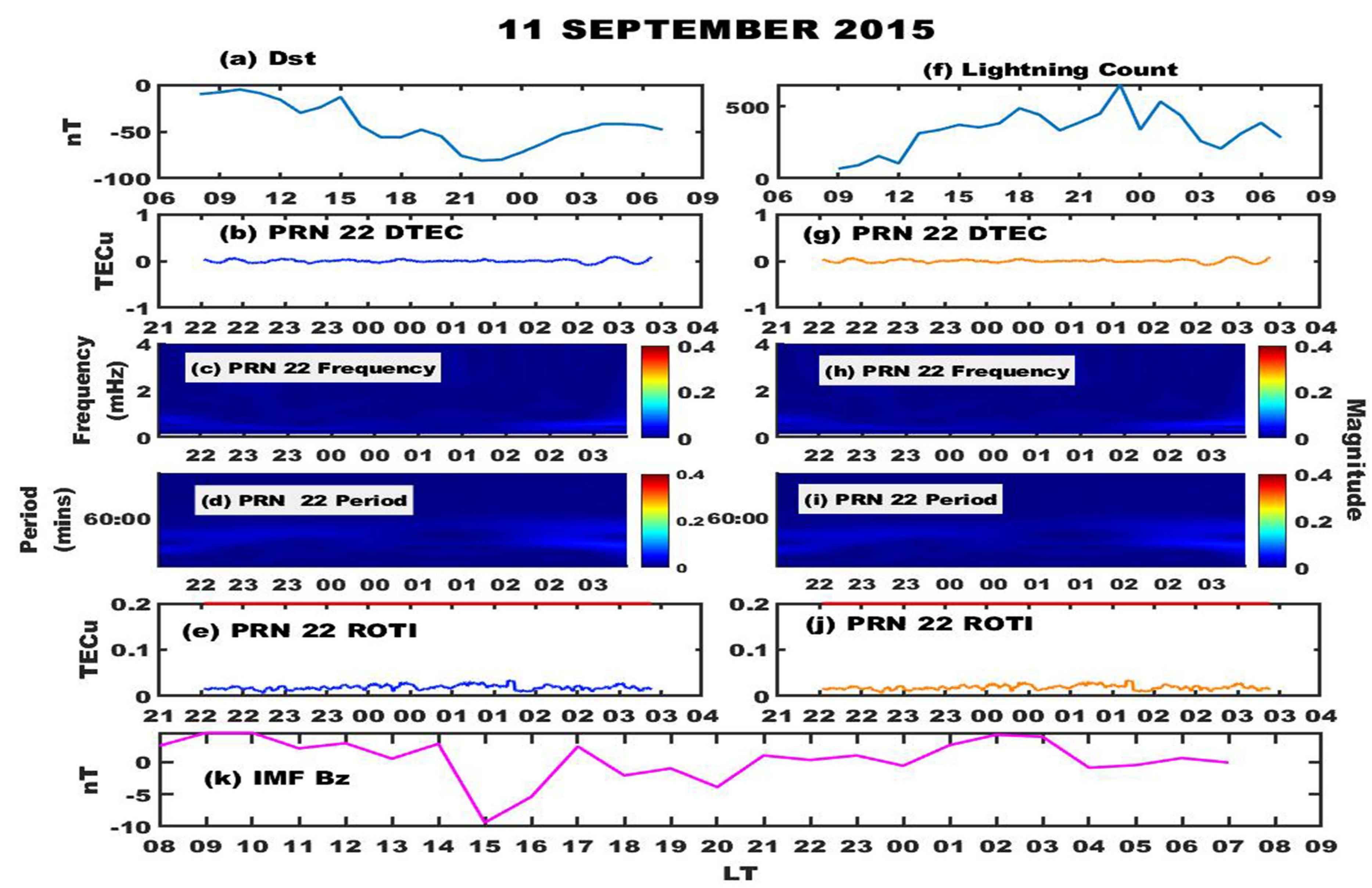

NO LIGHTNING - WEAK GEOMAGNETIC STORM (NL-WS)